SOIL STABILIZATION FIELD TRIAL

INTERIM REPORT

by

K.P. George

Conducted by the

DEPARTMENT OF CIVIL ENGINEERING
UNIVERSITY OF MISSISSIPPI

in corporation with

THE MISSISSIPPI DEPARTMENT OF TRANSPORTATION

U.S. DEPARTMENT OF TRANSPORTATION
FEDERAL HIGHWAY ADMINISTRATION

and

THE PORTLAND CEMENT ASSOCIATION

The University of Mississippi
University, Mississippi
April 2001

ABSTRACT

Shrinkage cracks in cement-stabilized bases/subbase can be alleviated by specifying the right cement dosage, or by other additives/procedures that suppress crack susceptibility. A field trial of six 1000 ft test sections to investigate several alternative techniques was initiated and constructed in August 2000. The following additives/procedures are included for investigation:

- Control group cement with 5.5% cement additive; design based on a reduced strength criteria.
- 5.5% cement precracked while "young".
- 5.5% cement precut (grooved) every 3m (10 ft).
- 3.5% cement with 8% fly ash.
- Ground granulated blast furnace slag (GGBFS) complemented by 2% lime.
- Three percent lime and 12% fly ash, the current favored stabilization technique of MDOT.

This interim report covers the tests and results conducted in three stages:

- Mixture design
- Construction monitoring
- Post-construction evaluation

The cement-treated material mix design was based on a low-strength criterion, namely, 7-day cured, 4-hour immersed strength of 2.0 MPa (290 psi) on ASTM recommended samples 71mm diameter and 142mm high (2.8 in diameter and 5.6 in high. Twenty-eight day strength of 2.4 MPa (350 psi) was used for cement-fly ash and lime-GGBFS combinations. In the precracked section, while the material was still gaining strength (24 hours after placing), a vibratory roller was employed to induce minute cracks in the layer. The uncompacted layer was precut at 3m (10 ft)

intervals, cuts filled with emulsion and compacted to density. MDOT's approved design of 3% lime and 12% fly ash was included as a master control section.

Large variations in density and moisture are recorded, attributable to inherent difficulties of in-place mixing and compacting. Though mix uniformity is satisfactory, field mixed material strength on average is 50% lower than that of laboratory mixed material. The stabilized material gained strength and showed substantial increase in modulus, due in part to extreme hot weather during and after construction. All of the sections, except lime-fly ash and precracked sections, underwent moderate cracking beginning as early as three days, and continued for 28 days (the reporting period), again due to persistent dry, hot weather. There is some indication that shrinkage cracking was aggravated by insufficient curing procedures, and more so in high strength materials.

Despite adverse weather conditions that prevailed during the construction as well as the first four weeks during which time the materials gained strength, the lime-fly ash treatment and precracking technique performed very well so far as shrinkage cracking is concerned. The reflection cracking potential of all six sections will be monitored for five years.

ACKNOWLEGMENT

This report includes the results of a study titled, "Soil Stabilization Field Trial," conducted by the Department of Civil Engineering, The University of Mississippi, in cooperation with the Mississippi Department of Transportation (MDOT) and the U.S. Department of Transportation, Federal Highway Administration.

The author wishes to thank Joy Portera, MDOT Research Engineer and Jan Prusinsky of Portland Cement Association for their technical input and encouragement in promoting the project study. Bill Barstis helped to organize the fieldwork and Johnny Hart organized the field data collection. The support of Holman Inc. (Tim Cost) is acknowledged here.

The excellent support provided by the MDOT Project Office, and District Office is acknowledged here. Special thanks to Jackie Harris, the project engineer and Danny Walker, the Assistant District Engineer. Hill Brothers Construction Company cooperated fully during the construction phase.

DISCLAIMER

The opinions, findings and conclusions expressed in this report are those of the author and not necessarily those of the Mississippi Department of Transportation or the Federal Highway Administration. This does not constitute a standard, specification or regulation.

TABLE OF CONTENTS

LIST OF TABLES

LIST OF FIGURES

CHAPTER 1

INTRODUCTION

1.1 BACKGROUND

A base/subbase course constructed of stabilized soil has many characteristics that contribute to the performance of the pavement. It has excellent load dispersion properties and is minimally affected by moisture. In addition, a stabilized base, by cushioning subgrade movement, preserves the integrity of the overlying pavement structure. The dosage of stabilizer to realize these benefits is often an issue, but one approach is that the end product should meet certain durability criteria. Occasionally, the dosage required to meet this criteria results in a rigid layer, which, if undergoes shrinkage, will develop cracks. In time, these cracks are likely to become wide. The result may be a reduction in the service life of the pavement owing primarily to water infiltration and/or reduction of load transfer across cracks.

The tendency to crack can be alleviated by controlling shrinkage (terminal) of stabilized soil and/or decreasing the rate of strength gain. Several additives are considered for decreasing the rate of strength gain of the stabilized material. Lime-fly ash (LFA), primarily for its slow-setting property, has been proven successful in stabilizing the abundant sand-clay material found in Mississippi. Cement Kiln Dust (CKD), a product of the cement industry, has been incorporated in an experimental project and its performance is currently being evaluated (1, 2). Ground granulated blast furnace slag (GGBFS), a by-product of the steel industry, is currently being considered either exclusively or in combination with cement and/or lime for soil stabilization. As with LFA, the crack performance of layers stabilized with either CKD or GGBFS is attributed to slow rates of cementitious reaction. One detrimental aspect of using LFA or GGBFS for stabilization is that the strength gain of the stabilized material is adversely affected by cold weather, thus substantially

reducing the length of the construction season. A comparative study of these stabilizers is warranted with special emphasis on early strength gain.

Portland cement has a proven record of providing a stable pavement base for thousands of miles of major highways in the United States and abroad; however, there is concern over possible shrinkage cracking due to drying and/or thermal contraction with time, especially in bases with a high percentage of this stabilizer. Recent studies suggest that crack-related degradation can be abated by adopting materials and/or methods that bring about a "desirable" crack pattern, "desirable" being defined as numerous fine cracks at close spacing, which ensures adequate load transfer across the cracks. It is not so much the number of cracks but the width of these cracks that has a significant influence on the long-term performance of the pavement since wider cracks have the tendency to reflect through the overlying pavement. Limiting/controlling drying shrinkage can effect the development of this "desirable" crack pattern in a stabilized layer. Several alternatives are available to control the drying shrinkage. These include: judiciously selecting the cement dosage, selecting a soil for stabilization having a limited fines content and plasticity, and the use of a fly ash additive in conjunction with Portland cement, all of which promote development of a "desirable" crack pattern in a stabilized layer. According to the Electric Power Research Institute, soil-cement base courses incorporating local soils with Portland cement and fly ash have been constructed in 17 states between the years 1975 and 1993.

Controlling shrinkage cracking is another method to alleviate the detrimental affects of this cracking to pavement performance. This control can be effected by "precutting" to induce a weak plane in the stabilized layer or "precracking" at an early age (before 48 hours after construction) by several passes of a vibratory roller with 100% coverage.

1.2 OBJECTIVES

In this study, a field trial was initiated to investigate various methods to alleviate the shrinkage cracking problem in cement stabilized layers. Incorporated in the field trial are the following materials or methods each in a separate but contiguous test section: cement, precut cement layer, pre-cracked cement layer, cement and fly ash, GGBF slag and lime and lime-fly ash (LFA). The scope of the study includes laboratory tests to design various mixtures, conduct quality control tests during construction of the sections and evaluate performance of these sections with special reference to shrinkage cracks in the base. In addition to evaluating the sections before asphalt overlay, monitoring would continue for five years studying reflected cracks, if any. Not only the absolute performance of each section will be studied, but the performance of the experimental sections will be compared with that of the LFA section. That the Mississippi Department of Transportation (MDOT) considers the LFA base an acceptable base is the primary reason for selecting this for benchmark performance. Based on overall performance of those five test sections with respect to the benchmark performance of LFA base, recommendations will be forthcoming to the Department as to the suitability of each material combination/process in base/subbase construction.

1.2.1 What Does This Interim Report Cover?

The various tasks undertaken before and during the field construction of the six test sections and a discussion of the results comprise this interim report. They include:

- Laboratory tests for mixture design of cement-treated soil and other additive combinations.
- Quality control tests (laboratory and field tests) during construction of the trial sections.
- Performance evaluation that includes in-place strength and stiffness, and most importantly, the evolution of cracks in the stabilized layer before overlaid by asphalt concrete.

•Tentative conclusions as to the performance of each section along with some recommendations for mix design and field construction.

CHAPTER 2

REVIEW OF LITERATURE

Soil-cement has many properties that recommend it as a flexible pavement base course. The perceived problems with cement stabilized base roads have generally stemmed from the tendency for discrete cracks within the base to propagate through the bituminous wearing surface – generally 38 to 152mm (1.5 to 6 in.) thick – giving rise to maintenance concerns. The first part of this chapter reviews the mechanics of cracks in the cement stabilized base and the second includes a discussion as to how these cracks reflect through the wearing surface.

2.1 MECHANICS OF BASE CRACKING

A cement stabilized pavement is comprised of a cement-treated base course with a bituminous wearing surface, either a surface treatment or a hot mix asphalt layer. The surface cracks that may appear could result from one or more of the following modes:

1. Reflecting shrinkage/thermal (environmental) cracks that originate in the cement base.
2. Reflecting load-induced fatigue cracks formed in the cement base due to heavy truck traffic.
3. Fatigue cracks induced at the bottom of the asphalt surface, eventually propagating to the surface.
4. Thermal cracks and cracks due to asphalt aging, both originating in the surface and eventually fracturing the asphalt layer.

With the exception of failure in the vicinity of shrinkage cracks, widespread fatigue along the wheel path of soil-cement pavement (item 2 above) is seldom a problem (3, 4, 5). Cracking in the bituminous surfacing is frequently associated with fatigue (item 3) and thermal contraction/aging (item 4). Literature exists on these two aspects of asphalt surface cracking (6).

Shrinkage cracks (item2), either due to drying or ambient temperature change, are inevitable in a cemented material. The cement stabilized layer shrinks due to drying, either from loss of moisture and/or "self desiccation" (moisture depletion resulting from cement hydration). It is argued that shrinkage cracking is a natural characteristic of soil-cement, signifying that the cement is producing a hardened base with significant flexural and tensile strength (7). Should the cracks become wider, however, degradation of the pavement along the cracks not only leads to a rough riding surface but also to delamination of the layers and local failure. The latter phenomenon is reinforced in recent studies (3, 4). For instance, Little, et al. (3) investigated the performance of several heavily stabilized bases, and concluded that the performance of the sections is dictated by the amount of shrinkage cracking. Wide shrinkage cracks have been singled out as a factor for premature degradation of soil-cement pavements. The wider the crack the more the water infiltration and consequent pumping of the underlying material. With the load-induced stresses increased along the crack edge, secondary cracks begin to appear, typically in the longitudinal direction along the wheel path.

2.2 MODEL FOR CEMENT BASE CRACKING

A simple model that emulates transverse cracks in a cement base has been developed by Rahim and George (8). The factors of importance for this simple one dimensional mechanistic model include:

- volume change (shrinkage) resulting from drying and/or temperature change;
- tensile strength of the stabilized material;
- stiffness and creep of stabilized materials; and
- the subgrade restraint.

With the assumption that the base maintains complete contact with the underlying layer, friction forces and resulting stresses are calculated and compared with the tensile strength of the cemented base. In long slabs, the friction forces become large enough to cause overstressing, resulting in a crack, theoretically in the middle of the slab. As drying shrinkage increases, the resulting stress also increases in the intact half-slab causing a second crack in the midsection. Successive cracks occur in the midsection of the remaining intact slabs, until the strength is not exceeded by the shrinkage stress. Simply put, this simple model asserts that the subgrade restraint induces tensile stress in the longitudinal direction of the slab, resulting in transverse cracks.

A parametric study, employing the model, yielded the following conclusions:

1. Ideal curing is beneficial so long as it can be assured until an asphalt surface is placed. Considering that the shrinkage cannot be eliminated, a logical recommendation is to place the asphalt surface as early as is practically feasible.
2. Controlling drying shrinkage of soil-cement indeed results in reduced cracking. Limiting the fines (plasticity index) in the soil is very effective in accomplishing this objective.
3. Increasing the subgrade resistance/adhesion promotes narrower crack width in soil-cement base. With the view to promote various layers to work together in the pavement system, it is imperative that full bond be assured at all the interfaces.
4. Additives that reduce the hardening rate have the potential of reducing cracking and/or crack width.

Shrinkage and/or thermal contraction comprise the primary causal factors of transverse cracking in cement treated base layers. Fine cracks initiated during the compaction procedure play a significant role as well. Resulting from the mismatch in stiffness and geometry between the soft and flat stabilized mixture and the rigid and round steel or pneumatic rollers, these hairline cracks

serve as seats for thermal crack initiation. A simplified analysis of roller-induced hairline cracks was presented by George (9), where it is shown that cracks initiated during compaction propagate in a series of steps due to drying shrinkage. Employing a finite element analysis, El Halim et al. (10) showed that vertical cracks originating from the top of the pavement, and propagating downwards through the thickness of the pavement layer or overlay would result in "lipping" along the edges of the crack from a slab curling effect. In contrast, a crack originating at the bottom (otherwise known as reflected cracks) and propagating upward results in cupping on the surface along the edges of the crack.

2.3 REFLECTION CRACKING IN THE WEARING SURFACE

Crack reflection through a road structure is one of the main causes of premature pavement deterioration. The discrete discontinuity introduced by the presence of the exiting crack tip in the underlying base layer results in the development of high tensile stress concentrations at the bottom of the overlay. These lead to the initiation and propagation of cracking into the overlay at a location directly above the existing crack (11). This type of cracking is commonly termed reflection cracking in the literature (see Figure 2.1.a).

Nevertheless, in some circumstances, depending on geometry and material properties cracking has been also observed to develop and propagate into the overlay from locations other than the tip of the existing crack. A prerequisite for these types of cracking is debonding between the overlay and the old pavement. For purposes of discussion, this type of reflection crack (see Figure 2.1.b) is designated secondary reflection cracking. Because of the multitude of parameters involved and the interplay between them, it is usually difficult if not impossible to determine a-priori, for a given pavement, which of the above two modes of cracking will prevail and what its implications will be on overlay deterioration.

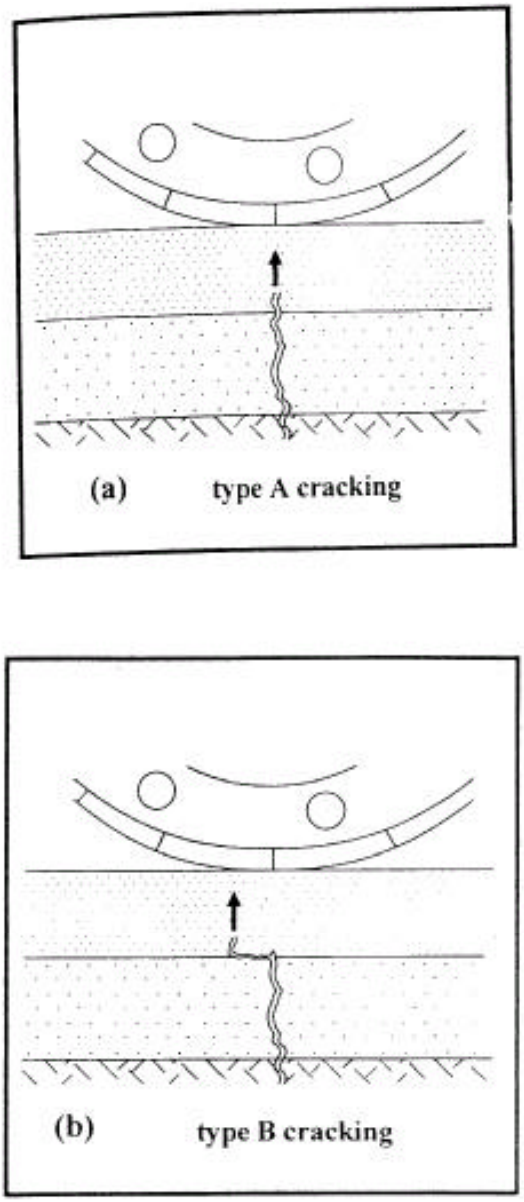

Figure 2.1 Types of cracking in pavement overlays(adopted from 11)

Quantitative studies investigating reflection cracking are few indeed. In an earlier field study conducted by MDOT (12), the crack density in the overlay was compared with that in the cement-treated base (the latter documented before constructing the overlay). The results were inconclusive to show a relationship between the base cracks and those reflected in the asphalt overlay.

A method to quantitatively predict the reflected cracks in an overlay incorporating the combined effect of cracked and un-cracked area in the underlying pavement/base is proposed in a recent paper (13). A basic assumption of this study is that the reflected cracked area follows a Gumbel distribution with respect to "damage," defined as the ratio of actual load repetitions to load repetitions needed for the crack to reach the surface. Suffice it to say that this attempt to quantify reflection cracking needs to be substantiated by controlled field studies.

2.4 MINIMIZING CRACKING IN CEMENT STABILIZED PAVEMENTS

Several procedures/techniques have been proposed for minimizing shrinkage cracks and resulting reflection cracking. A detailed description of those procedures can be found elsewhere (12, 13, 14, 15, 16, 17, 18, 19). For the purpose of this overview, they are grouped into four categories: First, controlling maximum shrinkage and consequent cracking by proportioning materials. Examples include use of minimum content consistent with long-term durability, specifying limiting fines content in the soil, and assuring practical minimum moisture during compaction, to name the important ones. Second, expansive cement, fly ash cement, or secondary additives such as fly ash and a host of other organic compounds have been proposed, again to reduce drying shrinkage (18). Quality construction, including maximum density close to proctor, proper curing and improving uniformity of mix fall under the third category. The fourth category addresses the issues directly by controlling shrinkage cracking in the stabilized

layer so that reflection cracking is minimized. Included in this fourth group are the following:

- Precracking the cement-stabilized base by delaying placement of surface;
- Precracking (mechanically) by immediately opening the base to traffic;
- Controlling cracking by precutting (18);
- Use of interlayers (surface treatment or stress relieving layers) inhibiting propagation of cracks from the base layer;
- Use of thicker asphalt concrete (AC) surface;
- Use of thicker base slab with reduced cement content, and;
- Prescribing material/methods (such as precracking) that promote numerous minute cracks (microcracks) in contrast to a few wide cracks.

The viability of these procedures in abating shrinkage cracks is discussed at length in a recent study (20). A technical memorandum was prepared incorporating causes and crack-related degradation. In order to gather up-to-date data on performance of in-service soil-cement pavements, a telephone survey of several State Highway agencies was conducted. This information was supplemented by studying the performance of soil-cement pavements in Mississippi. Several projects were inspected during and/or soon after construction. Pavements with cemented base that were included in the Long Term Pavement Performance database (LTPP, GPS sections from all over the nation) were also studied with special reference to cracking. A close scrutiny of the performance of those pavements from different sources suggests that crack-related degradation can be effectively mitigated by promoting numerous fine cracks in the base layer in contrast to few wide cracks.

The study recommended various mix combinations and construction techniques for accomplishing this "desirable" crack pattern. What follows is a brief review of how each of these procedures help to mitigate the cracking problem.

2.5 METHODS FOR MITIGATING CRACKS

2.5.1 Reduced Cement Content

Experiencing excessive shrinkage and resulting wide cracks, numerous highway agencies surveyed (reported in reference 20) have reduced the cement dosage from what could be required by durability consideration (such as wetting and drying test). Little et al. (3) investigated the performance of several heavily stabilized bases, and concluded that the performance of the sections is dictated by the amount of shrinkage cracking. Wider cracks, associated with high strength bases, allow water infiltration followed by debonding of layers and consequent pumping of the underlying material. The tenet is that by judiciously selecting the cement dosage, shrinkage can be abated to bring about numerous fine cracks at close spacing.

2.5.2 Precutting Cement Base

Originally introduced in France (21) the underlying principle of this technique is that by introducing grooves/cuts at close intervals (for instance, 10 feet apart) crack width can be controlled. Viewed differently, this technique is intended to prevent the occurrence of occasional but relatively wide and damaging natural cracks which can easily propagate through bituminous surfacing due to relative vertical movement of the crack edges under trafficking, therefore, necessitating thick bituminous surfacing. Benefits of precutting are described in reference 22 as well.

A controlled cracking study of a coarse grained soil-cement in U.K. (19) reported that the system effectively induced frequent cracks of less than 0.5 mm width in a cement bound base. The

width of natural cracking was more than 1.0 mm, depending upon the aggregate type. It was argued that the better performance of precut sections was due to superior aggregate interlock between the crack faces. It was also noted that the stiffness of a cement bound material (CBM) base is only slightly affected by controlled cracking, with minimal effect on the structural performance of the base. The French study (21) is even more convincing to show that precutting the base can considerably alleviate reflection cracking. As shown in Figure 2.2, the number of reflected transverse cracks in a 90 mm overlay is identical to that in a precut base with only 30 mm overlay, a substantial reduction in cost.

2.5.3 Precracking "Young" Soil-Cement

The basic promise of this procedure is that by precracking young soil-cement base, (by vibrating with a vibratory roller), numerous fine (hairline) cracks, which are not reflective, would be induced at close spacing. The first reported successful experiment of precracking by immediate traffic release was conducted in Japan (23), with encouraging results. An experimental section built in Mississippi (11), where the road was opened to traffic immediately, has performed better than a control section where traffic was redirected for a minimum of 7 days. Even more encouraging results are reported from Austria (24) where the cemented base was subjected to several passes of a 12-ton vibrating roller between 24 and 72 hours after construction. A comparison between deflection measurements before and after microcrack initiation shows an increase in the mean values, from 1.09 to 1.32 mm. Nevertheless, this increase of the mean values is reduced in the course of the setting process, suggesting healing of cracks.

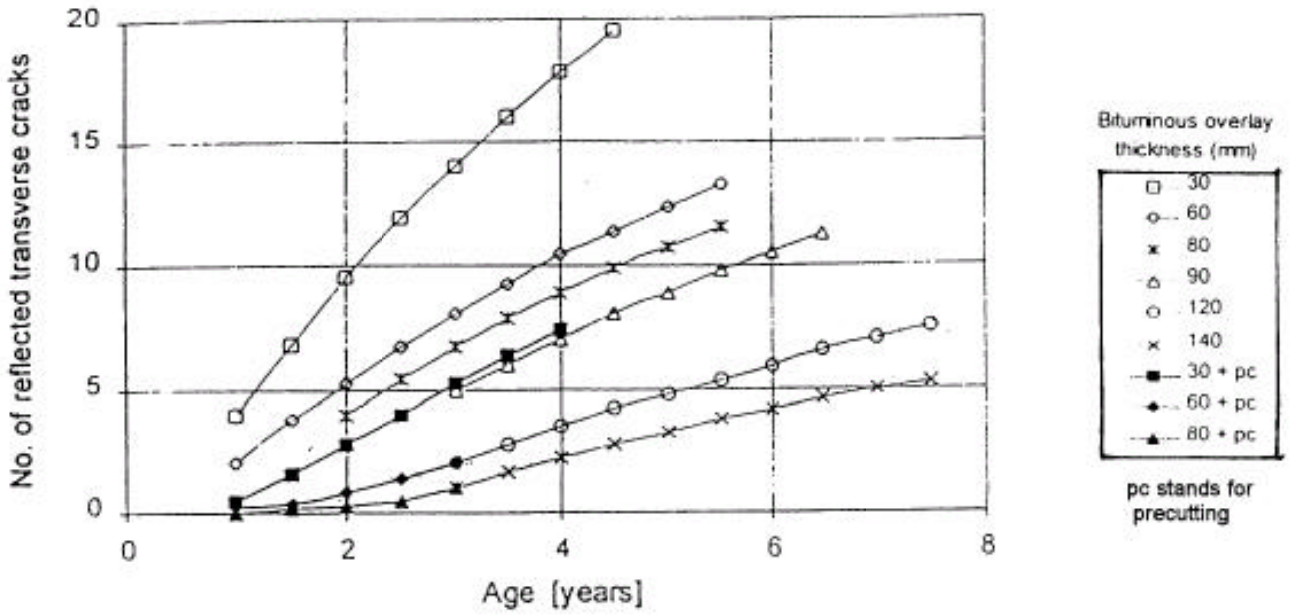

Figure 2.2 Crack reflection influenced by precutting the base (reference 19)

2.5.4 Fly Ash in Soil-Cement

One of the earliest laboratory studies of soil-cement by Davidson et al. (25) reported that fly ash addition increased the strength of the composite mixture by 28 percent. Fly ash has been used in cement-treated soils with encouraging strength results as well as satisfactory field performance (26). The Electric Power Research Institute cited various projects in which fly ash was used as an admixture with cement and lime (27). None of those studies attempted to evaluate the effectiveness of fly ash in reducing drying shrinkage and consequent cracking of base layers. The writer's laboratory studies indicate that cement fly ash mixtures decreased the drying shrinkage without sacrificing long-term strength (28). In addition, the setting (hardening) rate of cement fly ash mixture is curtailed, with consequent reduction in cracking. A PC-based model study clearly showed that, by replacing a part of the cement with fly ash, shrinkage cracks remain narrower than those occurring in bases with no fly ash admixture (8). The importance of narrower cracks has been reiterated in recent studies (4), where it is argued that long-term performance can be ensured by limiting the crack width.

2.5.5. Ground Granulated Blast-Furnace Slag

Though produced before dawn of the twentieth century, the use of GGBF slag as a separate cementitious material started in the 1950's. The composition of blast-furnace slag is determined by that of the ores, fluxing stone, and impurities in the coke charged into the blast furnace. Only to maximize cementitious properties, the molten slag is chilled rapidly, resulting in granulated (iron) blast-furnace slag. Typically, the slag is ground to an air-permeability (Blaine) fineness exceeding that of Portland cement.

The earlier use of GGBF slag was in replacing (typically) 50 percent of Portland cement in cement concrete. When GGBF slags are blended with cement, the combinations of cementitious material will result in physical properties that are characteristic of the dominant material. For example, as the percentage of GGBF slag increases, a slower rate of strength gain should be expected, particularly at early ages.

With the good track record of blast furnace slag concrete, slag and fly ash were used for base and subbase material for Indian Roads (29). The laboratory test results were encouraging. The Forest Service has used 30 percent lime activated GGBF slag in a test section and notes decreased strength gain, especially during the initial three months (30). Wollongong City Council has used blast furnace slag in combination with other materials for road construction (31). The authors reported good performance of 81 slag pavements laid between 1973 and 1980. In a 1998 study (32) in Thailand, the applicability of lime and GGBF slag combinations has been demonstrated.

In the test section proposed in this study, whether GGBF slag should be used in the presence of another cementitious material, for example, lime or fly ash, would be investigated prior to the mix design.

2.5.6 Lime-Fly Ash Stabilization

The use of lime-fly ash-aggregate mixtures in road construction has increased steadily since this mixture was introduced in the United States in the early 1950's. This material has gained acceptance with MDOT and it is now a standard material for base and subbase construction. Natural soils of a variety of textural composition have been successfully stabilized with lime and fly ash. When added to soil, it serves as a pozzolan and as a filler for voids. Pozzolanic reactions from which LFA mixtures derive their long-term strengths are influenced by many factors, including ingredient materials, proportions, processing, moisture content, field density, and curing conditions.

Both curing time and temperature greatly affect the strength and durability of "hardened" mixtures. In cold weather, the strength gain of the mixture is slow indeed. In an effort to accelerate development of early strength and improve the short-term durability characteristics of LFA mixtures, thereby permitting extension of the construction period later into the fall, admixtures (for example, Portland cement) have been added to accelerate or complement lime-fly ash reactions. The early strength development associated with hydration of Portland cement complements the slower strength development resulting from lime-fly ash reactions. Certain other admixtures (e.g. water-reducing agents) may also give beneficial results. However, the use of many admixtures may be impractical due to handling problems and additional costs. In order to take advantage of early strength development of Portland cement and long-term cementitious reaction of fly ash only, cement-fly ash admixture is considered an alternative to the LFA stabilization.

2.6 SUMMARY

This subject-specific review covers the following topics: How and why cement treated layers crack comprise the first section of the chapter. Mechanics of reflection cracks and a recent attempt to predict cracks are discussed in the second part of this chapter. Stressing the importance of various additives and/or procedures to minimize cracking, the review continued to discuss the underlying principle/mechanism responsible for abating cracks in stabilized pavement.

Described in the next chapter is the field trial undertaken to evaluate the effectiveness of some of the admixtures and procedures proposed for alleviating cracks in cement stabilized pavements.

CHAPTER 3

PROJECT SELECTION AND LABORATORY TESTS ON SOIL

3.1 PROJECT SELECTION

Several projects under contract were considered for the proposed experimental field trial. Six 305m (1000 ft) single lane test sections were to incorporate the following trials:

- Cement dosage ensuring reduced strength
- Controlled cracking by precutting
- Mechanical precracking by vibratory roller
- Cement-fly ash additive
- Lime-GGBFS additive
- Lime-fly ash (LFA) as control section

In selecting the project, uniform subgrade support was sought in the 1830 m (6000 ft) stretch of the road. Alternating cuts and embankments were avoided as much as possible. It was desired that asphalt overlay be placed soon after the preliminary condition survey was completed. The road project in Highway #302 in Marshall County, Mississippi was selected and negotiated with the contractor, Hill Brothers Construction Company, to build six test sections from station 190+00 to 250+00. A typical cross-section of the test pavement is presented in Figure 3.1, where the LFA base was replaced by five other stabilized layers. Twenty centimeters (8 inches) of Class 9, Group C material was to be trucked in, mixed thoroughly and stabilized with 3% lime and 12% fly ash, according to the original department plans. One thousand eight hundred thirty meters (6000 ft) of lime-fly ash subbase was to be replaced by six test sections, the parent material being class 9, group C. As cracks in the stabilized layers as well as reflective cracks are of interest in this study, the 10 cm (4 inch) thick crushed limestone drainable material was deleted from those test sections.

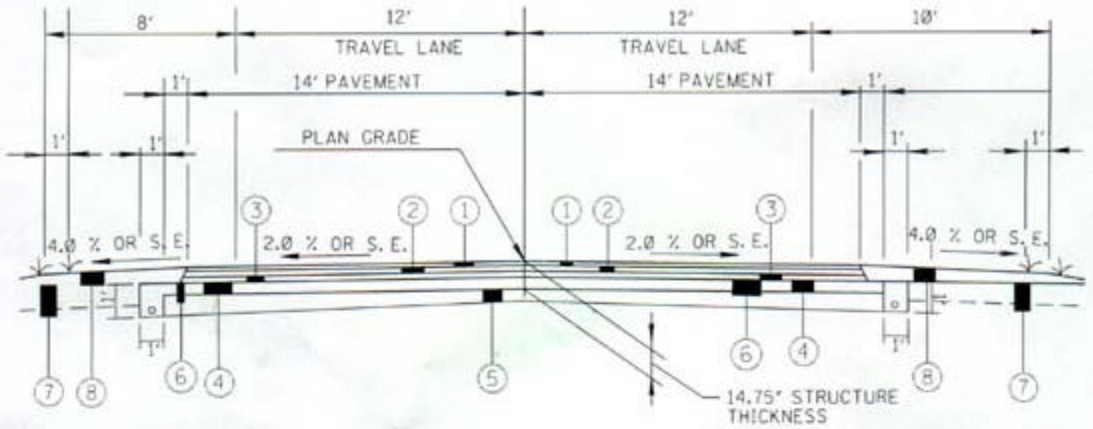

TYPICAL SECTION

① 2" HOT MIX ASPHALT, HT, POLYMER MODIFIED REQ'D. [1 @ 2" (12.5 mm MIXTURE)].

② 2.25" HOT MIX ASPHALT, HT, POLYMER MODIFIED REQ'D. [1 @ 2.25" (19 mm MIXTURE)].

③ 4.5" HOT MIX ASPHALT, HT, REQ'D. [2 @ 2.25" (19 mm MIXTURE)].

④ 6" LIME-FLY ASH BASE COURSE REQ'D. (INCORPORATED 3% LIME AND 12% FLY ASH INTO CL. 9, GROUP C, GRANULAR MATERIAL TO PRODUCE 6" COMPACTED LIME-FLY ASH COURSE)(30' WIDE).

⑤ 6" CHEMICALLY TREATED SUBGRADE REQ'D. LIME TREATED (4% LIME).

⑥ 6" GRANULAR MATERIAL (CL. 9, GP. C) REQ'D. •SEE NOTE.

⑦ 12" & VAR. GRANULAR MATERIAL (CL. 9, GP. C) REQ'D.

⑧ 8.75" & VAR. GRANULAR MATERIAL (CL. 3, GP. D) REQ'D.

• THE DESIGN SOIL WAS GRADED TO 2% CROSS SLOPE 15' LT. & RT. OF CENTER LINE THROUGHOUT PROJECT.

FIGURE 3.1 TYPICAL TEST SECTION X- SECTION, MISSISSIPPI HIGHWAY #302, MARSHALL COUNTY

3.2 SOIL TESTS

Representative samples of the class 9, group C material from each test section were collected from the road for classification, followed by mix design tests. As will be shown all of the six samples were practically identical, as they all came from the same borrow pit.

3.2.1 Classification Tests

Particle size distribution (AASHTO T88-90) and Atterberg limit tests (AASHTO T89-90 and T90-87) were conducted on six samples with the results presented in Table 3.1. All of the samples were nonplastic and classified A-2-4 (AASHTO M145). Moisture density relationships of the soils with various admixtures, namely, cement in sections 1, 2, and 3, cement-fly ash in section 4 and lime-GGBFS in Section 5 are determined in accordance with AASHTO T99 and the results are tabulated in columns 8 and 9 of Table 3.1.

3.2.2 Mix-Design Tests:

As cement dosage is shown to be a crucial element in controlling cracks, a thorough literature search was conducted which led us to a tentative strength criterion. Presented in Appendix A1 is the logic in selecting strength criteria. Accordingly, the cement dosage needs to be determined using the criterion of 2.0 MPa (290 psi) compressive strength in a 7 cm (2.58 inch) diameter 14 cm (5.6 inch) high sample, cured for 7 days at 72ºF followed by 4 hours of water immersion. A sample with height to diameter ratio of 2:1 (herein referred to as ASTM size) is preferred (29) for strength tests, in contrast to the Proctor-size samples routinely used by many agencies. The MDOT standard operating procedure, MT-25 entitled “Design of Soil-Cement Mixtures” stipulates Proctor-size samples. As discussed in Appendix A1, laboratory tests on cement-treated soil indicates that Proctor sample strength is approximately 30% larger than that of ASTM size samples.

Table 3.1 Classification test results including optimum moisture and density.

Section No.	Station No.	Admixture / Treatment	Additive Propotion by weight	Passing No. 200, %	Liquid Limit (L.L), %	Plasticity Index (PI)	Maximum Density, pcf [a]	Optimum Moisture, %
1	190 - 200	Cement	5.5%	10.3	-----	NP	118.5	11.7
2	200 - 210	Cement/ Precracked	5.5%	12.3	-----	NP	118.5	11.7
3	210 - 220	Cement/ Precut	5.5%	9.8	-----	NP	118.5	11.7
4	220 - 230	Cement and Fly ash	3.5%Cement 8% Flyash	13.5	-----	NP	121.9	10.3
5	230 - 240	Lime and GGBFS	2% Lime 6% GGBFS	12.4	-----	NP	119.0	11.0
6	240 - 250	Lime and Fly ash	3%Lime 12%Flyash	13.6	-----	NP	118.9	10.2

[a] 1 pcf = 0.1571 kN per cu. m.

[b] Original section stations that were subsequently modified during construction.

The mix design tests in the laboratory were conducted employing ASTM size samples, with side-by-side tests conducted on Proctor samples, for comparison purposes.

3.2.2.1 *Cement Dosage for Class 9, Group C Soil*

ASTM samples in triplicate were molded at cement contents of 3.5%, 5% and 6.5%, then cured and tested in accordance with ASTM D1633. For comparison purposes, Proctor samples were also cast and tested (as per MT-25) using three different cement contents. From the plot of unconfined compressive strength against cement dosage (see Figure 3.2), the cement required for 7-day strength of 2.0 MPa (290 psi) in ASTM size sample is 4.5%. This project being a field trial of short sections, and realizing that the contractor had limited experience in cement stabilization work, a larger cement content of 5.5% was recommended for the cement stabilized sections.

3.2.2.2 *Mix Design of Cement-Fly Ash Mixture*:

A rule of thumb for selecting the additives when using both cement and fly ash is to replace 2% of the cement with fly ash (class C); cement replacement at 1:4 ratio. Accordingly, the preliminary design called for 3.5% cement and 8% class C fly ash. Whether this combination of additives satisfies the strength criterion is verified by strength-testing two mixtures: first, 3.5% cement and 8% fly ash and second, 4% cement and 8% fly ash. Prior to strength testing, the samples were submerged in water for 4 hours in accordance with the ASTM test procedure. Figure 3.3 compares the strengths of the two additive combinations to note that the 3.5% cement (with 8% fly ash) provides the required 28-day strength of 2.4 MPa (350 psi) in ASTM-size samples. (The rationale for selecting 350 psi is included in Appendix A1). In fact, the strength of the 4% cement plus 8% fly ash mixture is well above the criterion, and hence not considered any further. Comparing the strengths of ASTM size samples with the Proctor Samples (see Figures 3.3), it is noted that the Proctor

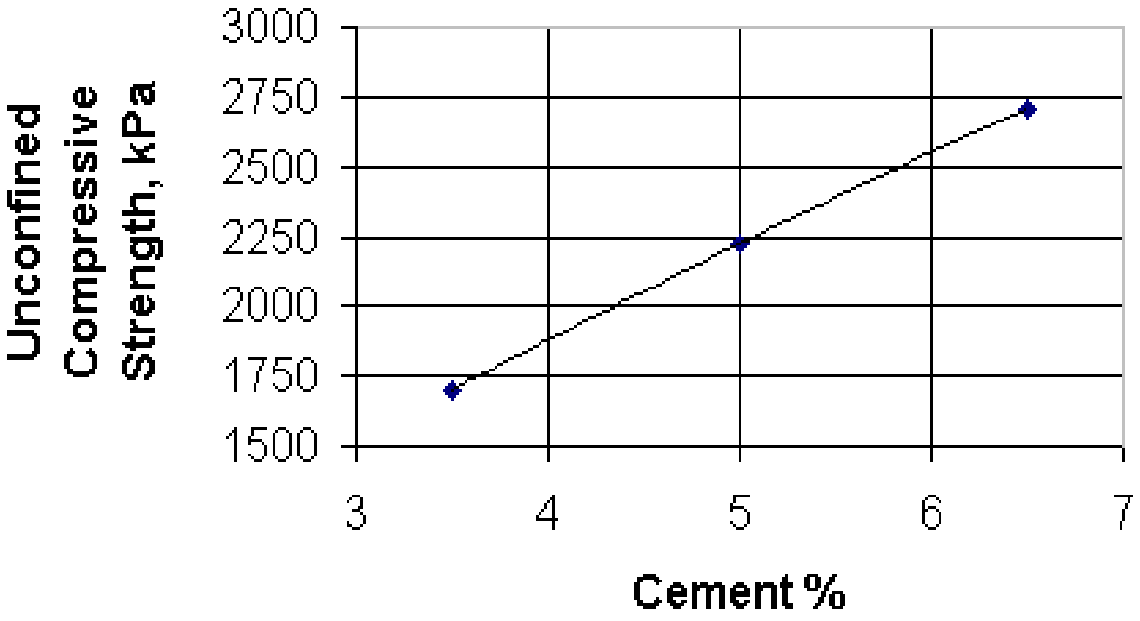

Figure 3.2 Compressive strength vs cement dosage. 1 kPa = 0.145 psi

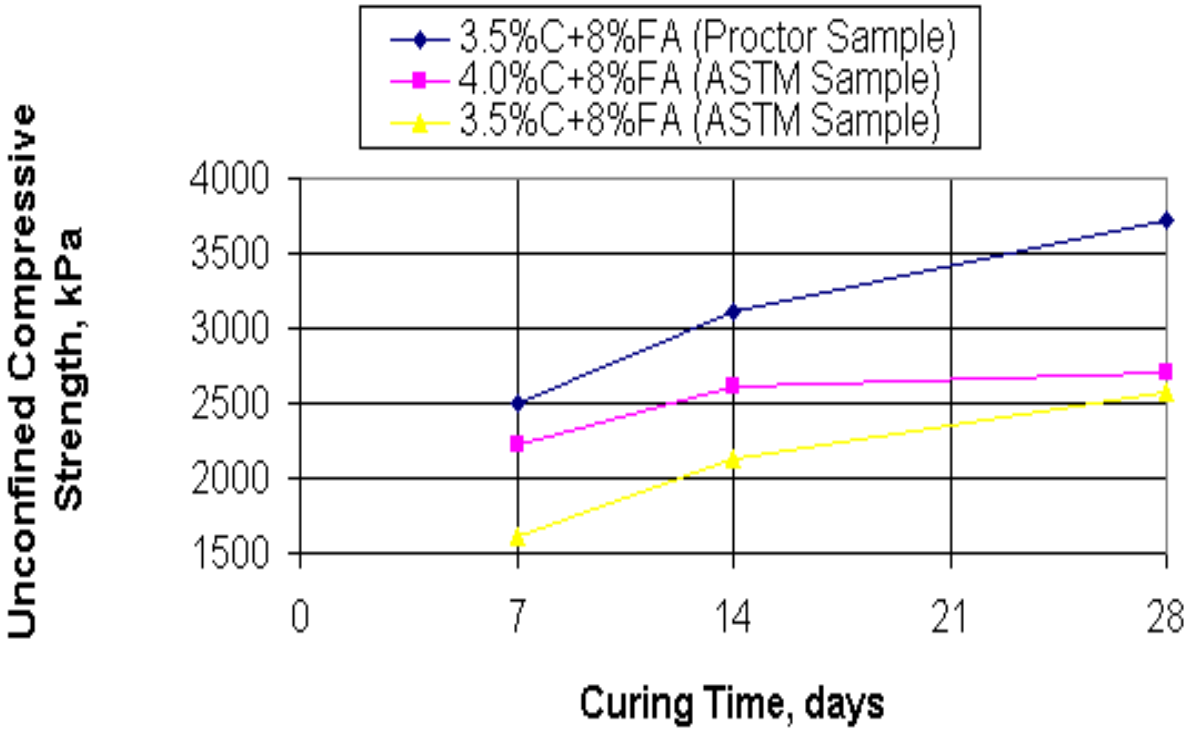

Figure 3.3 Compressive strength increase with time. 1 kPa = 0.145 psi

samples are on average 30% stronger than the ASTM counterparts. Recommended additives, therefore, amount to 3.5% cement and 8% fly ash.

3.2.2.3 *Mix Design of Lime – GGBFS Mixture*

The strength criterion used is the same as that used in cement-fly ash mixture, namely 28-day strength of 2.4 MPa (350 psi). Two mixture combinations were tested and strength results are presented in Figure 3.4. GGBFS alone failed to provide a mixture of the required strength. As can be seen 2% lime and 5% GGBFS mixture tested at 2.3 MPa (334 psi), close to 2.4 MPa (350 psi) criterion. Again, in order to offset any unforeseen problems in the field construction and consequent strength loss, a slightly conservative mix, namely, 2% lime and 6% GGBFS is chosen for the test section.

The consequence of adopting a relatively high strength mixture will be discussed in light of crack results discussed in chapter 5.

3.2.2.4 Mix Design of Lime-Fly Ash-Control Section

MDOT has routinely used lime-fly ash for base/subbase stabilization. The MDOT LFA mix design strength criterion is 3.4 MPa (500 psi) subsequent to a 28-day accelerated curing period and a five-hour soak time in water. Following this criterion, MDOT specified 3% lime and 12% fly ash. Note that the entire Highway #302 was to receive this treatment. As the primary objective was to compare the performance of the trial sections with that of MDOT's standard, the control section was built with admixture percentages of 3% lime and 12% fly ash.

3.3 SUMMARY

This chapter presented the project selection criteria and the routine test results on the bulk samples collected from the six test sections. Employing a modified strength criterion, mix proportions were determined; either with cement alone, cement and a secondary additive such as

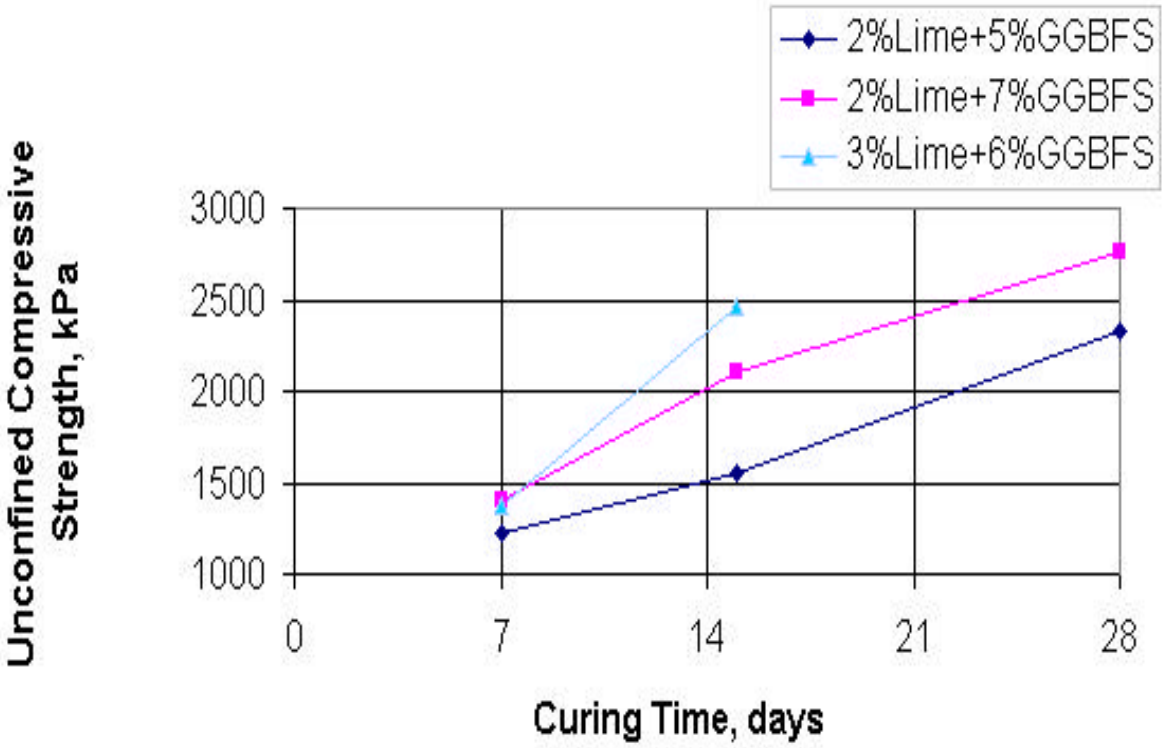

Figure 3.4 Strength gain of various Lime-GGBFS mixtures with time. 1 kPa = 0.145 psi

fly ash or lime and GGBFS. The standard MDOT design proportions were adopted for the lime-fly ash control section.

CHAPTER 4

CONSTRUCTION AND MONITORING OF TEST SECTIONS

The original plan called for constructing six 1000 ft. test sections contiguously from 190+00 to 250+00. Some modifications to this plan were mandated during construction, which will be described in a later section of this chapter. What follows are the section locations as they exist in the field:

190+00 to 195+00: cement 5.5%, control cement, Section 1A

215+00 to 220+00: cement 5.5%, control cement, Section 3A

200+00 to 210+00: cement 5.5%, precracked, Section 2

195+00 to 200+00: cement 5.5%, precut, Section 1B

215+00 to 220+00: cement 5.5%, precut, Section 3B

220+00 to 230+00: cement 3.5% and fly ash 8%, Section 4

230+00 to 240+00: lime 2% and GGBFS 6%, Section 5

240+00 to 250+00: lime 3% and fly ash 12%, Section 6

4.1 FIELD CONSTRUCTION OF STABILIZED LAYER

The sand clay (Class 9, Group C) was brought in and placed during early summer of 2000. Subsequently, in each test section the applicable additive was spread, mixed in place and compacted to specified density.

Work started on 8/17/00, beginning from station 220+00, proceeding westward. When a single admixture was administered for mixing, the following compacting and finishing steps were generally followed:

Step 1. One or two passes of dry mixing, employing a rotary mixer to incorporate the additive, such as cement (see Figure 4.1)

Figure 4.1 Dry mixing soil and lime employing a rotary mixer.

Step 2. Water added (water quantity is approximated) (see Figure 4.2)

Step 3. One or two passes of wet mixing, as required (see Figure 4.3)

Step 4. Several passes of vibratory sheepfoot roller, until the roller walks out (see Figure 4.4)

Step 5. Blading with a motor grader and final compaction with one or two passes of a rubber-tire roller (see Figure 4.5)

Step 6. Finish grading with a motor grader after grade stakes were driven every 15m (50 ft) to render the necessary cross-slope

When two admixtures, for example, cement and fly ash were added, an initial mixing of one of the additives (fly ash in this case) with soil was accomplished using a disc attached to a tractor. After adding cement the dry mixing using the rotary mixer followed. In general, the contractor chose to work in 152m (500 ft) sections when cement additive was used and 304m (1000 ft) sections with lime additive.

What follows are the time-lines and some of the special features and/or problems during construction.

4.1.1 Precut Section: 215+00 to 220+00 (Section 3B) and Cement Section: 210+00 to 215+00 (Section 3A)

The original plan for the 304m (1000ft.) precut test section was to subdivide it into 2-152m (500ft.) subsections. One of these subsections was to be precut before compaction and the other subsection was to be precut after compaction. The original plan location of this entire test section was to be between stations 210+00 and 220+00. Due to problems encountered during construction, one of the subsections was located between stations 215+00 and 220+00 and the other subsection was located between stations 195+00 and 200+00. The construction of the subsection between the

Figure 4.2 Water being added to the dry-mixed soil and additive(s).

Figure 4.3 Wet-mixing of soil and additive(s).

Figure 4.4 Initial compaction by sheeps-foot roller.

Figure 4.5 Finish-compaction by rubber-tired roller.

latter two stations will be discussed in 4.1.3 Precut Section: Station 195+00 to 200+00 (Section1B).

Subsequent to dry mixing the cement in the soil, water was added to Section 3B at 8:45 AM. The material was mixed again and bladed with a motor grader. The desired groove depth for this precutting technique is one-half the thickness of the stabilized layer and the desired groove width at the top of the groove is 10mm (3/8 inch). Several techniques were attempted to cut the grooves in the loose material. These included a motor grader blade, a modified bulldozer blade and a modified motor grader blade. The first two techniques, the motor grader blade and the modified bulldozer blade, were eliminated because both of these methods created an excessively wide groove. The width at the top of the groove made with the motor grader blade was almost 50mm (2 inches).

The original plan called for cutting and filling the grooves without any prior compaction of the mix and allowing the subsequent compaction process to close the grooves together as the material underwent densification. While evaluating the various techniques for actually cutting the grooves it was observed that the material was sloughing off the sides of the groove. To rectify this sloughing problem, two passes of the rubber tire roller were made to sufficiently tighten, but not completely compact, the material prior to further cutting of the grooves.

The transverse oriented grooves were cut on a 3.0m (10 ft.) interval along the length of the subsection. The third technique, a modified motor grader blade, was successfully employed to cut these grooves. A disk blade, or rotary cutter, 410mm (16 inches) in diameter and 10mm (3/8 inch) in thickness was devised by the contractor and mounted on one end of the motor grader blade (Figure 4.6).

The depth of the groove was controlled by the experienced motor grader operator. The groove width made with this device was somewhat in excess of 13mm (½ inch) at the top of the

Figure 4.6 Grooves being cut in partially compacted layer employing a rotary blade.

groove, exceeding the desired groove width. Should this technique be adopted as a standard construction method, it is recommended to reduce the thickness of the rotary cutter.

The contractor filled the grooves with an EPR-1 emulsion that was applied through a nozzle attached to a distributor truck (Figure 4.7). Both the groove cutting and groove filling operation was completed in about 50 minutes for this 152m (500 ft.) subsection. This subsection was then lightly bladed with the motor grader to fill in the grooves, sprinkled with water and then rolled with two passes of the rubber tire roller to complete the compaction process. The final rolling was completed at 11:00 A.M.

A cut was made across one of the grooves to examine how well the compaction operation had closed the groove. It was observed that the material in the groove was somewhat soft, primarily due to excess emulsion. Cutting the narrower desired groove width would have reduced the amount of emulsion required to fill the groove while still developing the desired vertical discontinuity within the stabilized layer.

The segment of road from station 210+00 to 215+00 was supposed to be precut after compaction of the subsection. This subsection was to be compacted to the final design density and then the grooves cut and filled with EPR-1 emulsion. The grooves would then be closed with a final pass of the rubber tire roller. The desired groove width is 5mm (3/16 inch) for this precutting technique. This is less than that required for the previous technique since closing widths in excess of 5mm (3/16 inch) by rolling on fully compacted material will not effect adequate closure of the grooves.

This subsection was watered, mixed and fully compacted prior to attempting any precutting operation. The contractor attempted to use a concrete saw to cut the grooves (Figure 4.8). Two problems became apparent as the sawing operation proceeded which resulted in the termination of

Figure 4.7 Grooves being filled with emulsion.

Figure 4.8 Grooves being cut in compacted layer employing a concrete saw.

this groove cutting technique. One problem was that the width of the grooves exceeded the 5mm (3/16 inch) requirement. The other problem was the length of time needed for the sawing operation. Based on the time required to cut several grooves with the concrete saw, it was estimated that more than two and one-half hours would be required to complete the sawing of this subsection. This would result in almost four hours elapsing between wet mixing to final rolling to close the grooves. Any closure of the grooves from final rolling that long after wet mixing would be detrimental to the stabilized material; therefore, attempts were discontinued to use this segment of road as a precut test subsection.

This section was designated a control cement subsection. To obtain a total of 304m (1000 ft.) as a control cement section, this 152m (500 ft.) subsection was complemented by another 152m (500 ft.) cement control subsection located between stations 190+00 and 195+00.

The concrete saw was the only option considered for cutting grooves subsequent to complete compaction of the soil cement layer. Since this method proved to be inadequate, the precut after compaction technique to effect the "desired crack pattern" in the stabilized layer was eliminated from the study. The subsection between stations 195+00 to 200+00 was subsequently constructed with the precut before compaction technique.

4.1.2 Precracked Section: Station 200+00 to 210+00 (Section 2)

After adding water at 11 AM, this section was successfully mixed, compacted and finished in two hours and 15 minutes. The surface of the section was kept moist for 24 hours from multiple passes of the water truck. At the end of this moist curing period, four passes of an 8.8 ton vibratory roller were made on the section to induce microcracks in the material. Subsequent to rolling the section was sealed with a curing membrane.

The speed and vibration frequency of the vibratory roller were arrived at by trial and error. Requiring impulses to be imparted to the surface at 4 inches apart, we selected a roller speed of 5 kmh (3 mph, 264 ft/min) and a roller frequency of 800 vibrations per minute (vpm). The vibrator made available had only two settings, low and high. Our subjective judgment was that the low frequency setting yielded an approximate frequency of 800rpm. The spacing of impulse, therefore, would calculate to (244 ft/mm/800rpm) 10 mm (0.33 ft).

The issue of number of passes of the vibratory roller was determined by monitoring the reduction in modulus of elasticity with the number of coverage. Five sample locations were monitored with the geogauge to observe that, on average, the loss in modulus was nearly 25% after four passes of the 8.8 ton roller. Figure 4.9 shows the vibratory roller in operation. Four passes of the roller were required to realize on average a 25% reduction in modulus. Modulus before and after precracking is plotted in Figure 4.10. Geogauge employed in modulus determination is shown in Figure 4.11. The surface being somewhat brittle, because of the extreme hot weather, began to scab, limiting the number of passes to four. One recommendation here would be to apply the curing seal soon after construction in order to alleviate the scabbing problem.

The surface before precracking had a few fine shrinkage cracks, however, they were practically invisible because of the loose sand particles on the surface. No more surface cracks appeared even after four passes of the vibratory roller. Therefore, we attribute the decrease in modulus to microcracks induced in the material, rather than to structural cracks. The latter type is indeed undesirable from the point of view of long-term performance of the stabilized layer.

Figure 4.9 Vibration roller in operation precracking the layer after 24 hours.

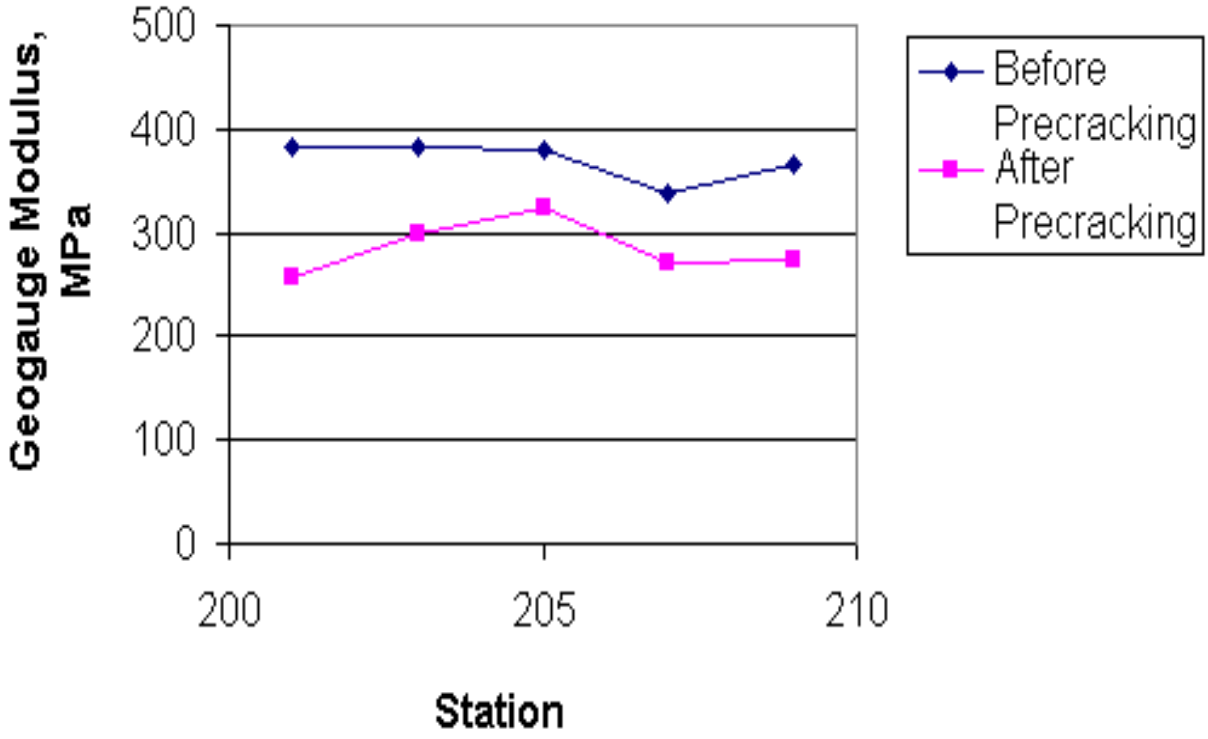

Figure 4.10 Modulus before and after Precracking.

Figure 4.11 Geogauge in operation evaluating modulus of layer in-place.

Figure 4.12 Cross section through a precut joint filled with emulsion.

4.1.3 Precut Section: Station 195+00 to 200+00 (Section 1B)

Per the discussion in section 4.1.1, this section was constructed with the precut before compaction technique. Now having some experience with this procedure, the contractor was able to shorten the time elapsed from adding water to the mix to filling the grooves with emulsion. The water was added at 1:45 P.M. with the completion of these steps in one hour and 45 minutes.

While the construction of Section 1B was progressing, density testing was performed in Sections 3B and 3A. The results of these density tests indicated that an adequate level of compaction had not been achieved in these sections; therefore, the contractor slightly modified the construction sequence of this section (1B) subsequent to the groove filling operation. Recall that in the first precut section (3B) the groove filling operation was followed by blading the section to fill the grooves with loose material and then rolling with the rubber tire roller. In the current precut section (1B) the contractor rolled the section with one pass of the 8.8 ton vibratory roller subsequent to the groove filling operation but before blading the section with the motor grader.

The section was bladed and then water was applied to the surface. An excess amount of water was placed as evidenced by the pumping of some of the grooves in the design lane. This area was again bladed and then compacted with two passes of the rubber tire roller.

A post-mortem examination (Figures 4.12 and 4.13) revealed that the joints were not adequately closed following this construction sequence. Two potential explanations include not blading the surface soon after filling the grooves with emulsion and the inadvertent addition of excess water before adequately closing the grooves with stabilized material. An overall view of the finished surface can be seen in Figure 4.14.

Figure 4.13 Close-up view of a precut joint.

Figure 4.14 Visible precut joints after final grading and compaction.

4.1.4 Cement Section: Station 190+00 to 195+00 (Section 1A)

The last 152m (500 ft) of the first day's construction was a cement subsection (designated 1A), where again 5.5% cement was added, dry mixed, water added, compacted and final grade established. No special problems were experienced in this section.

Note that the high temperature of the day (8/17/00) was 102? F with 100% sunshine.

4.1.5 Cement – Fly Ash Section: 220+00 to 230+00 (Section 4)

Work started in this section on 8/18/00, with an overcast sky and predicted high of upper 90's as compared to 102? F the day before. Fly ash was added and disked into the soil, which subsequently received a dry mixing using a rotary mixer after application of the cement admixture. The road surface was bladed, water added and again wet mixed with a rotary mixer. A second water application was required to bring the mixture to optimum moisture, which then was compacted with a vibratory sheepsfoot roller followed by a rubber tired roller.

The mixing and compaction operations progressed as expected with no special problems. Not only did the mix look very uniform, the workability of the mix was excellent as well. Wet mixing started at 9:00 AM, the surface was finished at 11:30 AM and curing compound applied by 12 noon.

4.1.6 Lime-GGBFS Section: Station 230+00 to 240+00 (Section 5)

Similar to the cement-fly ash section, a two-stage mixing procedure was used for this test section. The GGBFS was disked into the soil, the lime applied and then this mix was dry mixed with a rotary mixer. Water was applied to this section at 11:45 A.M. Upon completion of wet mixing and partial compaction by the sheepsfoot roller, the mixture appeared dry and non-uniformly mixed as evidenced by the appearance in several places where the virgin soil had not received any stabilizing agent.

A second water application and another wet mixing was completed by 2:15 P.M., which corrected these deficiencies. Final compaction was accomplished with the rubber tire roller. Grading and finishing to desired levels was completed without any major problems by 2:45 P.M. Time for wet mixing to finishing the 304m (1000 ft.) section was approximately 3 hours.

4.1.7 Lime – Fly Ash Section: 240+00 to 250+00 (Section 6)

Fly ash was added to dry soil followed by disking the soil-fly ash mixture. Lime was subsequently incorporated by dry mixing with a rotary mixer. Wet mixing with the same equipment followed after water addition. The material was bladed and subsequently compacted with two passes of a sheepsfoot roller. Having observed that the mix remained dry, water was added a second time and remixed and compacted, first with a sheepsfoot and second a rubber tired roller. The mix appeared wet after the second watering. The surface was now graded to true levels and recompacted with a rubber tired roller. Mixing and laying down time, namely, from wet mixing to compaction to final grade, for the 304m (1000 ft) section was approximately 2 hours and 30 minutes.

A special note is in order here regarding the climate during the two days of construction. The high temperatures were $102^{?}$ F and $94^{?}$ F, respectively, on 8/17 and 8/18 with 100% sunshine. This could have caused rapid cement hydration, undesirable from the point of view of shrinkage cracking. To what extent these extreme temperatures' affected cracking is not precisely known.

This being an experimental project, additional Proctor samples were molded for laboratory testing, some in-place densities besides the standard density and moisture tests conducted, and sieve tests of mixed material for uniformity of mixing taken. The results of the special tests are presented in the ensuing section.

4.2 MONITORING TESTS DURING CONSTRUCTION AND RESULTS

Owing to difficulties encountered during construction, the control section and the precut section were each built in two 152m (500 ft) lengths. With these modifications, the following section designation is used throughout this report.

- 190+00 to 195+00: cement 5.5%, cement control – Section 1A
- 195+00 to 200+00: cement 5.5%, precut – Section 1B
- 200+00 to 210+00: cement 5.5%, precracked - Section 2
- 210+00 to 215+00: cement 5.5%, cement control - Section 3A
- 215+00 to 220+00: cement 5.5%, precut - Section 3B
- 220+00 to 230+00: cement 3.5% and fly ash 8% - Section 4
- 230+00 to 240+00: lime 2% and GGBFS 6% - Section 5
- 240+00 to 250+00: lime 3% and fly ash 12%, MDOT Standard - Section 6

In order to circumvent the variations in the finished subbase that might occur in transitioning from one section to another, the two end lengths, 30m (100 ft) each of 304m (1000 ft) sections and 15m (50 ft) each for 152m (500 ft) sections, were not monitored, leaving the section lengths to 244m (800 ft) and 122m (400 ft) respectively. Sample locations 61m (200 ft) apart were located in each section resulting in 5 locations in 244m (800 ft) sections and 3 locations in 122m (400 ft) sections. During the construction of the test sections, the following investigations were conducted and they are discussed in the following sections, along with results, as appropriate.

4.2.1 Stabilized Soil Samples for Strength

From each sample location, a sample of stabilized soil was collected and Proctor samples molded. From six test sections a total of 48 samples were molded in the field laboratory (see Table 4.1). Before casting the cylinders, the moisture content of the composite sample was determined by a Speedy Moisture

Meter. With the weight and moisture content known, the dry unit weight of each sample could be calculated.

The cylinders, wrapped to prevent moisture loss, were transported to the laboratory for moist curing. Approximately a third were cured for 7 days, and a second third for 14 days and the rest 28 days before testing them in accordance with ASTM D 1633-84. As specified in the ASTM test procedure, the samples were immersed in water for four hours before testing. Density, moisture and strength results of the samples are listed in Table 4.1.

These strength results will be compared with those of the laboratory mixed and laboratory compacted samples, delineating the effect of mix efficiency on strength.

4.2.2 In-Place Density By Sand Cone

Employing a sand cone, unit weight (interchangeably designated density, mass/unit volume) of the compacted (finished) stabilized layer was determined, again one test at each sample location. Unit weight results and corresponding moisture contents of all the sample locations are presented in Table 4.2. It is well known that the strength of stabilized material is strongly dependent upon the unit weight and the molding moisture, accordingly, the in-place density could become useful in analyzing the compressive strengths of cores extracted 28 days after construction.

4.3 POST CONSTRUCTION EVALUATION TESTS

Following completion of the six test sections, various tests were planned, primarily to measure the stiffness (modulus), crack density, and strength of stabilized material. In-place tests were conducted periodically, determining the modulus of the stabilized layer and, in turn, assessing the progress of cementitous reaction. Surface cracks were monitored and mapped by manual survey. Four-inch cores were extracted and tested for unconfined compression strength. Figure 4.15 shows core drilling in progress.

Table 4.1 Compressive strength results along with moisture and density of Proctor samples molded from field mixed material.

Section No.	Location	Moisture, %	Percent Density	Curing, days	Strength, kPa [a]
1A [b]	191+00	9.9	92.7	7	1330
	193+00	10.1	92.2	7	1060
	193+00	10.1	93.7	14	1340
1B [b]	195+50	11.1	93.0	7	860
	195+50	11.1	95.0	28	1070
	197+00	9.6	90.5	7	950
	197+00	9.6	92.2	28	1000
	199+00	8.3	93.2	14	920
2 [b]	201+00	7.3	90.8	7	650
	203+00	8.9	93.9	7	1410
	203+00	8.9	92.8	14	1660
	205+00	9.3	91.1	7	710
	205+00	9.3	92.7	28	1170
	207+00	10.6	89.5	7	1220
	207+00	10.6	90.6	28	1650
	209+00	12.1	94.5	14	3020
3A [b]	211+00	9.8	91.8	7	950
	213+00	10.6	89.0	7	1190
	213+00	10.6	87.0	14	1260
3B [b]	215+00	10.8	88.8	7	1020
	215+00	10.8	101.5	28	1490
	217+00	13.3	97.9	7	2340
	217+00	13.3	97.9	28	2950
	219+00	13.4	99.6	14	2350
4 [c]	221+00	9.6	90.2	7	990
	223+00	9.1	95.3	7	690
	223+00	9.1	94.8	14	1040
	225+00	12.1	92.7	7	430
	225+00	12.1	92.6	28	720
	227+00			14	890
	227+00			28	940
	229+00	12.3	94.7	14	1090
5 [d]	231+00	13.6	98.5	7	1200
	233+00	12.3	100.8	7	1830
	233+00	12.3	101.0	14	2690
	235+00	8.8	99.9	7	680
	235+00	8.8	101.7	14	1230
	235+00	8.8	99.2	28	2180
	237+00	10.4	94.2	7	1020
	237+00	10.4	93.3	28	1490
6 [e]	241+00	14.8	96.6	7	230
	243+00	9.6	98.2	7	280
	243+00	9.6	102.9	14	260
	245+00	9.8	102.1	7	390
	245+00	9.8	101.1	28	1270
	247+00	12.4	99.3	7	310
	247+00	12.4	98.4	28	280
	249+00	11.8	97.3	14	200

[a] 1kPa = 0.145 psi

[b] Percent of maximum density (118.5 pounds per cu. ft.)

[c] Percent of maximum density (121.9 pounds per cu. ft.)

[d] Percent of maximum density (119.0 pounds per cu. ft.)

[e] Percent of maximum density (118.9 pounds per cu. ft.)

Table 4.2 Sand cone density and moisture content of in place compacted materials.

Section No.	Location	Moisture, %	Percent Density [a]
1A	191+00	10.1	93.6
	193+00	13.7	93.6
1B	195+50	13.9	96.6
	197+00	11.6	104.5
	199+00		
2	201+00	8.3	91.7
	203+00		
	205+00	7.8	83.8
	207+00		
	209+00	10.1	94.6
3A	211+00		
	213+00		
3B	215+00	7.8	91.7
	217+00	7.3	81.8
	219+00	8.3	79.8
4	221+00	7.9	89.5
	223+00		
	225+00	9.8	92.0
	227+00		
	229+00	10.0	93.6
5	231+00	12.3	91.8
	233+00		
	235+00	11.3	94.1
	237+00	13.8	92.9
	239+00		
6	241+00		
	243+00	8.1	76.1
	245+00		
	247+00	9.6	81.7
	249+00	12.8	92.8

[a] Percent of maximum density (118.5 pounds per cu.ft)

Figure 4.15 Core drill in operation.

4.3.1 Modulus of Stabilized Layer Employing Geogauge

In-place testing devices such as geogauge and Falling Weight Deflectometer devices were employed periodically. Geogauge is a device that induces vibration on the surface and picks up the resulting force and deformation to calculate the stiffness from which moduli can be calculated using an empirical correlation. A complete description of geogauge can be seen in reference (30). Geogauge moduli were determined at each sample location at 4, 7, 14 and 28 days after construction. These moduli are tabulated in Table 4.3.

Four days prior to stabilized layer construction (8/14/00), the lime-treated subgrade was tested in five sample locations 61m (200 ft) apart, with the modulus values tabulated in column 3 of Table 4.3.

As explained in section 4.3.5, in view of the significantly different performance of the first half of section 6, the adjacent 152m (500 ft) section, designated 6 alternate, was added, and 14 and 28 day moduli reported in Table 4.3.

4.3.2 Falling Weight Deflectometer (FWD) Study

MDOT Research Division staff facilitated the FWD deflection measurements seven and 28 days after construction. Deflection measurements were conducted at every 30m (100 ft) along each test segment, and a few special measurements in the vicinity of precut grooves, the purpose being to evaluate the load transfer efficiency (LTE) of the discontinuity. The FWD in operation is shown in Figure 4.16. The following test setup was used in the FWD tests: three seating drops at drop height 1, one peak test record at drop height 1 and second peak record at drop height 2. A total of two test measurements were, therefore, recorded at each test location. For brevity FWD deflection data will not be included in this report, however, the backcalculated modulus of each test location is reported and discussed in chapter 5.

Table 4.3 Modulus determined employing Geogauge on treated subgrade and on the subbase layer.

Section No.	Location	Modulus, MPa a				
			Stabilized layer			
		Lime Treated Subgrade	4 Days	7 Days	14 Days	28 Days
1-A	190+50	190	310	260	250	220
	192+50	160	400	270	230	340
	194+50		430	430	390	300
1-B	195+50	250	420	360	430	350
	197+50	220	400	250	300	240
	199+50	310	380	350	330	280
2	201	400	340	230	210	150
	203	250	410	350	410	320
	205	270	150	130	110	240
	207	230	230	170	210	190
	209	190	270	190	220	170
3-A	210+50	270	380	220	230	210
	212+50	210	490	340	280	190
	214+56		360	360	370	210
3-B	215+50	190	270	300	220	170
	217+50	470	230	170	140	210
	219+50	430	360	280	220	240
4	221+05	230	450	420	320	300
	223+05	340	340	330	360	280
	225+05	250	310	310	320	340
	227+05	160	360	380	270	190
	229+05	200	390	300	310	200
5	231+05	200	440	310	370	340
	233+05	90	420	360	340	370
	235+05	120	350	300	280	310
	237+05	90	250	270	250	250
	239+05	190	370	340	280	310
6	241+05	300	270	320	290	240
	243+05	150	170	230	220	190
	245+05	150	230	310	300	150
	247+05	300	140	150	160	180
	248+95	190	230	180	160	210
6 Alternate	250+50				260	210
	251+50				160	190
	252+50				170	220
	253+50				200	200
	254+50				290	170

a 1 MPa = 0.145 ksi.

Figure 4.16 Falling Weight Deflectometer in operation.

4.3.3 Crack Mapping

All surface cracks (primarily longitudinal and transverse) were mapped at seven, 17 and 28 days after construction. Cracks were manually surveyed, categorized into four groups – fine and low, medium and high severity – and sketched in grid paper in the field. The following classification was adopted for low, medium, and high severity:

Fine – width of crack less than 1mm

Low – width of crack = 1mm and < 2mm

Medium – width of crack = 2mm and < 3mm

High – width of crack = 3mm

Figure 4.17 is a view of the survey crew at work.

Special weight factors were introduced aggregating the four different severity levels. Weight factors assumed were 1, 0.75, 0.5 and 0.2 for high, medium, low severity and fine cracks, respectively. Assuming the crack effects a 0.3m (one foot) wide strip, crack area is calculated and total cracks expressed in percent (100 * area cracked/area of section), designated crack density. A sample calculation of crack density can be seen in Appendix A2. Figure 4.18 graphs crack survey results up to 28 days after construction.

What follows is a series of pictures from the five sections captured during the 14-day survey. Random, medium severity cracks in the control cement subsection (190+00 to 195+00) can be seen in Figure 4.19. In Figure 4.20, the transverse crack is medium severity in comparison to low severity longitudinal cracks, again in Section 1A. In the Precut Section 1B (195+00 to 200+00), however, the cracks were predominately in the transverse direction with a few longitudinal cracks as well. Very few cracks appeared in the precracked section (200+00 to 210+00), as attested to by the almost crack-free surface in Figure 4.21. Again, random cracks,

Figure 4.17 Survey crew measuring and mapping cracks.

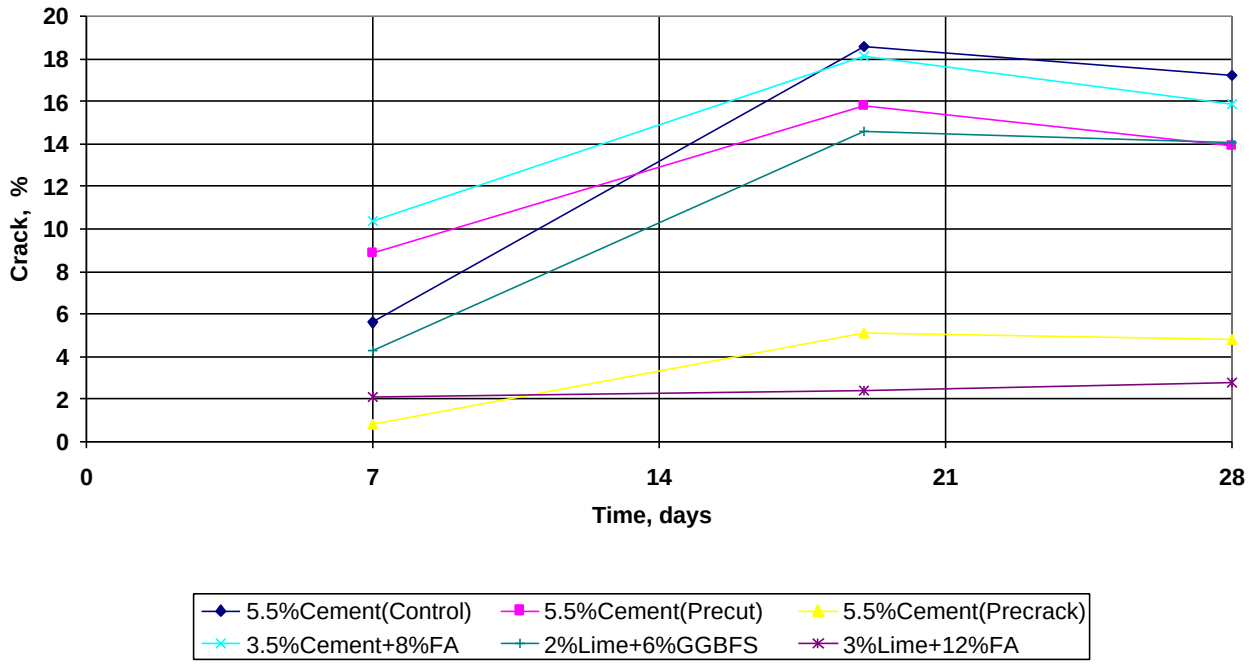

Figure 4.18 Increase of crack density with time.

Figure 4.19 Medium severity cracks in section 1A, control cement, fourteenth day.

Figure 4.20 Medium transverse and low longitudinal cracks in section 1A, control cement, fourteenth day.

Figure 4.21 Crack-free surface of section 2 (precracked), fourteenth day.

similar to those observed in section 1A, covered the complementary control cement, subsection 3A (200+00 to 205+00) (see Figure 4.22). For reasons not yet clear, the cracks in the cement-fly ash section appeared slightly more severe than those in the control cement section, as captured in Figure 4.23. Owing to excessive moisture during compaction, the first third of the LFA section (240+00 to 243+00) underwent severe cracking. What is shown in Figure 4.24 is typical block cracking observed in this segment of the LFA section. Typical cracks in the LFA section were of low severity and Figure 4.25 attests to this conclusion. With the cracks in the first third of the LFA section drastically different from what has typically been observed in the second half and also in adjacent LFA sections, a decision was made to substitute the first 152m (500 ft) by another segment of equal length, beginning at 250+00 and ending at 255+00. This 152m (500 ft) section is designated section 6 alternate. What is shown in Figure 4.26 is a view (westward) of the two subsections, constructed on two different days – the lighter surface in the background is the tail end of the original LFA section 6 (240+00 to 250+00) and the dark surface in the foreground portrays the new segment (245+00 to 250+00). Partly owing to better curing, the cracks in the well-cured half were much less than those observed in the poorly cured former half (background versus foreground). Based on this result, the author cannot overemphasize the importance of adequate curing in abating shrinkage cracks.

4.3.4 Strength of Stabilized Layer

In-place strength of the stabilized layer was determined employing a Clegg Impact Soil Tester, indirectly determining compressive strength. The Clegg hammer consists of a 10-lb compaction hammer together with a guide tube and an electronic meter. The meter signal is provided with an accelerometer fastened to the hammer. The deceleration readout, designated Clegg hammer impact value (CIV), is correlated to compressive strength. A typical correlation is

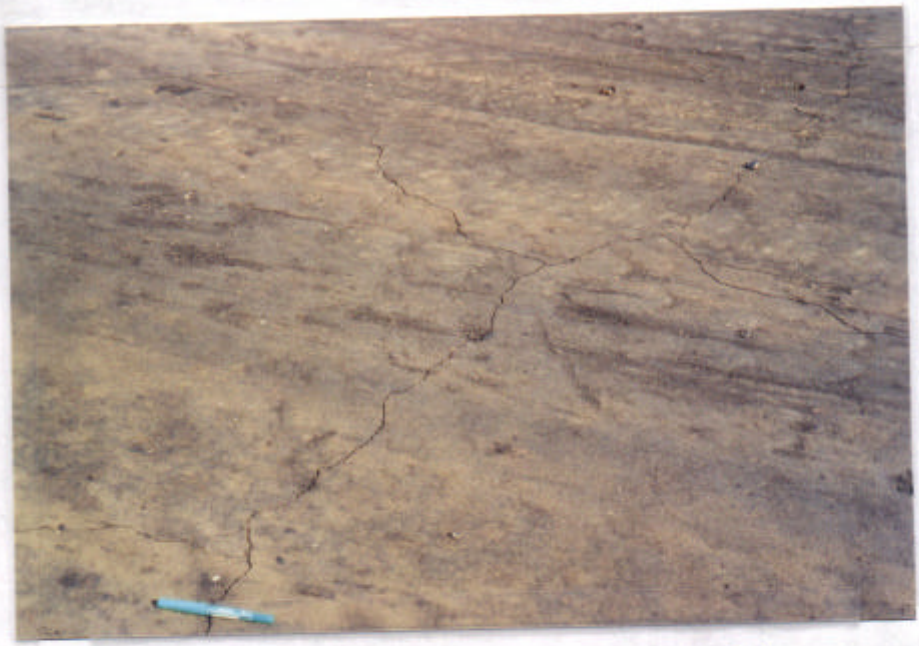

Figure 4.22 Random cracks in section 3A, control cement, fourteenth day.

Figure 4.23 High severity cracks in section 4, cement-fly ash, twenty-eighth day.

Figure 4.24 High severity cracks in section 6, lime – fly ash, 241 + 50, fourteenth day.

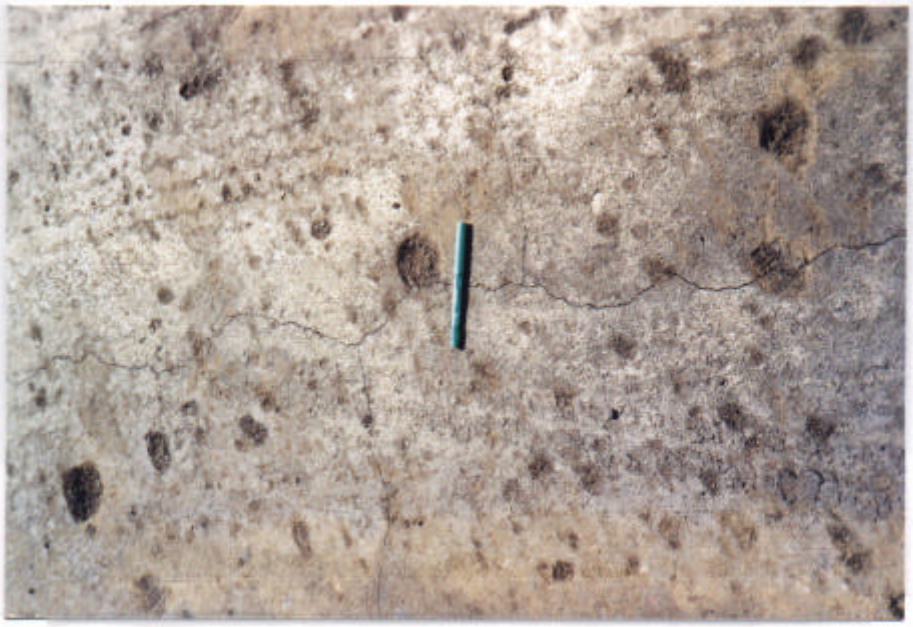

Figure 4.25 Typical crack in lime – fly ash section, 189 + 50, approximately twentieth day.

Figure 4.26 Comparison of emulsion retained, section 6 (alternate) in the foreground and section 6 in the background, fourteenth day.

presented in Figure 4.27 (31). Figure 4.28 is a view of the test in progress, with geogauge on the left and the Clegg hammer on the right. This impact-testing device, despite not being recognized as a standard test, was beneficial in evaluating the strength gain of stabilized material as time progressed. Note that at early stages, good cores could not be obtained. Clegg hammer strength values obtained at four, seven and 28 days are tabulated in Table 4.4.

Four-inch diameter core samples were obtained 28 days after construction. Again, one core was extracted from each sample location providing five cores in a 244m (800 ft) section. Cores were wiped dry before testing them in the laboratory, in order to minimize the effect of water used in drilling. Note that the cores were capped with plaster of paris before testing for strength, in accordance with ASTM D1633-84. The cap thickness was kept as minimum as possible, on average 10mm (3/8 inch). The unconfined compressive strength of field cores can be seen in Table 4.4 and repeated in Table 4.5. With sample height close to 4.6 inches, the strengths are reported without making a correction for height to diameter ratio.

A few field cores were tested in compression with deformation measurement, enabling the calculation of static modulus of the respective stabilized material. These results, presented in Table 4.5, will be compared with those obtained from Geogauge and FWD.

4.4 Summary

This chapter includes a description of construction of the test sections, a few problems encountered during construction, the results of monitoring tests designed to ensure quality, and finally the monitoring/evaluation test results for the first 28 days since completion of construction. The results compiled will now be analyzed, interpreting the performance of the various sections during the initial period of 28 days.

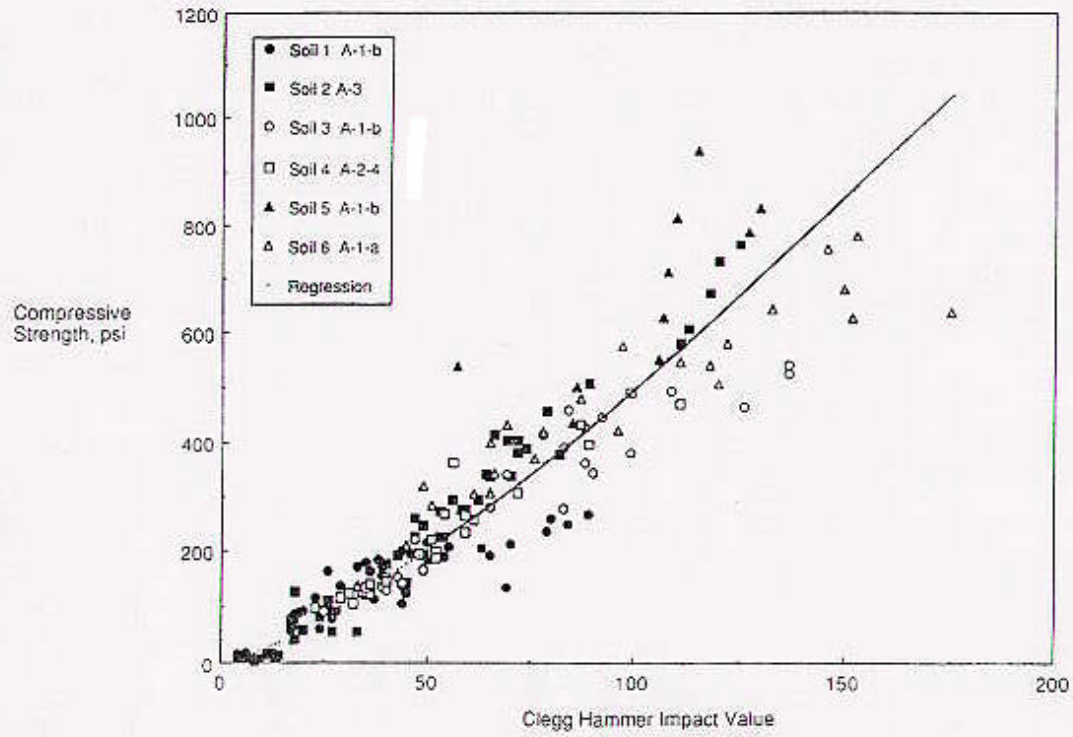

Figure 4.27 Compressive strength correlated to Clegg impact value (Adopted from 31).

Figure 4.28 View of geogauge (left) and Clegg impact hammer (right).

Table 4.4 Clegg hammer and field core strengths at 4, 7 and 28 days compared to those of field mixed laboratory compacted samples.

Section	Station	Strength, kPa [a]						
		Clegg Hammer				Field Mixed Lab Compacted		
		4 Days	7 Days	28 Days	Field cores 28 Days	7 Days	14 Days	28 Days
1-A	190+50	1270	1560	1830	1280 [b]	1330		
	192+50	1890	2190	2130	720	1060	1340	
	194+50	2220	3340 [b]	2370	750		1340	
1-B	195+50	2700	2610	2010		860		1070
	197+50	2250	2200	1600	1390	950		1000
	199+50	2070	2260	1180	1240		920	
2	201+00	1480	1020	2910	1310	650		
	203+00	3650 [b]	4260 [b]	1290	890	1410	1660	
	205+00	1280	1440	1030	580	710		1170
	207+00	870	950	1270	500	1220		1650
	209+00	1650	1680	1510	1120		3020	
3-A	210+50	1600	1900	1250	660	950		
	212+50	1680	1520	1150	690	1190	1260	
	214+56	2190	1920	1060	720			
3-B	215+56	1100	1350	1040	630	1020		1490
	217+55	1000	1140	2360	670	2340		2950
	219+55	1790	1800	3670 [b]	1430		2350	
4	221+05	3970 [b]	3500 [b]	1940	1270	990		
	223+05	1720	1930	1900	760	690	1040	
	225+05	1580	1810	1680	990	430		720
	227+05	1720	2080	2130	870		890	940
	229+05	1760	1910	2570	680		1090	
5	231+05	2630	2780	4040	3740	1200		
	233+05	3000	3440 [b]	3160	1550	1830	2690	
	235+05	2940	2860	1510	1880	680	1230	
	237+05	1770	2830	1600	730	1020		2180
	239+05	2010	2570	1100				1500
6	241+05	1120	1640	1060		230		
	243+05	920	1300	1130		280	250	
	245+05	980	1520	990	240	390		1270
	247+05	700	880	870		310		280
	248+95	780	790	940			200	
6 Alternate	250+50		740	900	230			
	251+50		630	1870 [b]				
	252+50		710	1020				
	253+50		860	1130				
	254+50		910	1060	440 [b]			

[a] 1 kPa = 0.145 psi

[b] Outlier tested according to Chauvenet's criterion

Table 4.5 Compressive strength of field cores corrected for height and static modulus of selected samples at 28 days.

Section	Location	Strength of Core, kPa [a]	Static Modulus, MPa	Modulus-Strength Ratio
	190+50	1280 [b]	330	258
	192+50	720	90	125
1-A	194+50	750	180	240
	195+50			
	197+50	1390		
1-B	199+50	1240		
	201+00	1310	160	122
	203+00	890	120	135
	205+00	580	70	121
	207+00	500	180	360
2	209+00	1120	110	98
	210+50	660	250	379
	212+50	690		
3-A	214+56	720	230	319
	215+56	630	170	270
	217+55	670	120	179
3-B	219+55	1430	330	231
	221+05	1270	370	291
	223+05	760	360	474
	225+05	990	240	242
	227+05	870	290	333
4	229+05	680	150	221
	231+05	3740 [b]	650	
	233+05	1550	280	181
	235+05	1880	270	144
	237+05	730	220	301
5	239+05			
	241+05			
	243+05			
	245+05	240		
	247+05			
6	248+95			
	250+50	230		
	251+50			
	252+50			
	253+50		100	310
6 Alternate	254+50	440 [b]		

[a] 1kPa = 0.145 psi

[b] Outlier tested according to Chauvenet's criterion

Chapter 5

FIRST PHASE MONITORING RESULTS AND DISCUSSION

The first phase results comprise those obtained during construction of test sections, and those compiled during the initial period of 28 days since construction. After which the stabilized layer was covered with hot mix asphalt (HMA) concrete. Of particular interest during construction are the density and strength of field-mixed material, which will be compared with those from the laboratory-prepared specimens assessing the mix uniformity attainable with typical mixing operation. The preliminary monitoring results include in-place modulus determination, the crack survey and strength tests in place and on field cores as well. These results are discussed comparing the performance of the five test sections.

5.1 CONSTRUCTION MONITORING TESTS

5.1.1 Compressive strength of stabilized material – Laboratory Prepared versus Field Mixed

Compressive strengths of laboratory-mixed, laboratory-compacted proctor samples are compared with those of the field-mixed field-laboratory casted cylinders (see Table 5.1 and Figure 5.1). As expected the field mixed material strengths are lower than the laboratory mixed counterpart, 30 to 50% lower depending on the mix combination. Non-uniform distribution of both stabilizing agent and water could be the important causal factors for the strength decrease. Delay of compaction in the field – average delay one to two hours – may be another reason for the loss of strength.

It should be remarked that the Mississippi Department of Transportation (MDOT) specifications call for the field mixed material to be devoid of large lumps, requiring at least 80% of the mixed material passing through a #4 sieve. The Class 9 material being non-plastic, the

Table 5.1 Comparison of compressive strengths of laboratory prepared and field mixed Proctor cylinders.

Section No.	Station	Strength, kPa [a]					
		7 Day strength		14 Day strength		28 Day strength	
		Lab [b]	Field	Lab [b]	Field	Lab [b]	Field
1A	191+00	2160	1330	2670		2700	
	193+00		1060		1340		
1B	195+50	2160	860	2670		2700	1070
	197+00		950				1000
	199+00				930		
2	201+00	2160	650	2670		2700	
	203+00		1410		1660		
	205+00		710				1170
	207+00		1220				1660
	209+00				3020		
3A	211+00	2160	950	2670		2700	
	213+00		1190		1260		
3B	215+00	2160	1020	2670		2700	1490
	217+00		2340				2950
	219+00				2350		
4	221+00	1620	990	2120		2580	
	223+00		690		1040		
	225+00		430				720
	227+00				890		940
	229+00				1090		
5	231+00	1300	1200	2490		3080	
	233+00		1830		2690		
	235+00		680		1230		2180
	237+00		1020				1490
	239+00						
6	241+00		230				
	243+00		280		260		
	245+00		390				1270
	247+00		310				280
	249+00				200		

[a] 1 kPa = 0.145 psi

[b] Average strength, bulk samples.

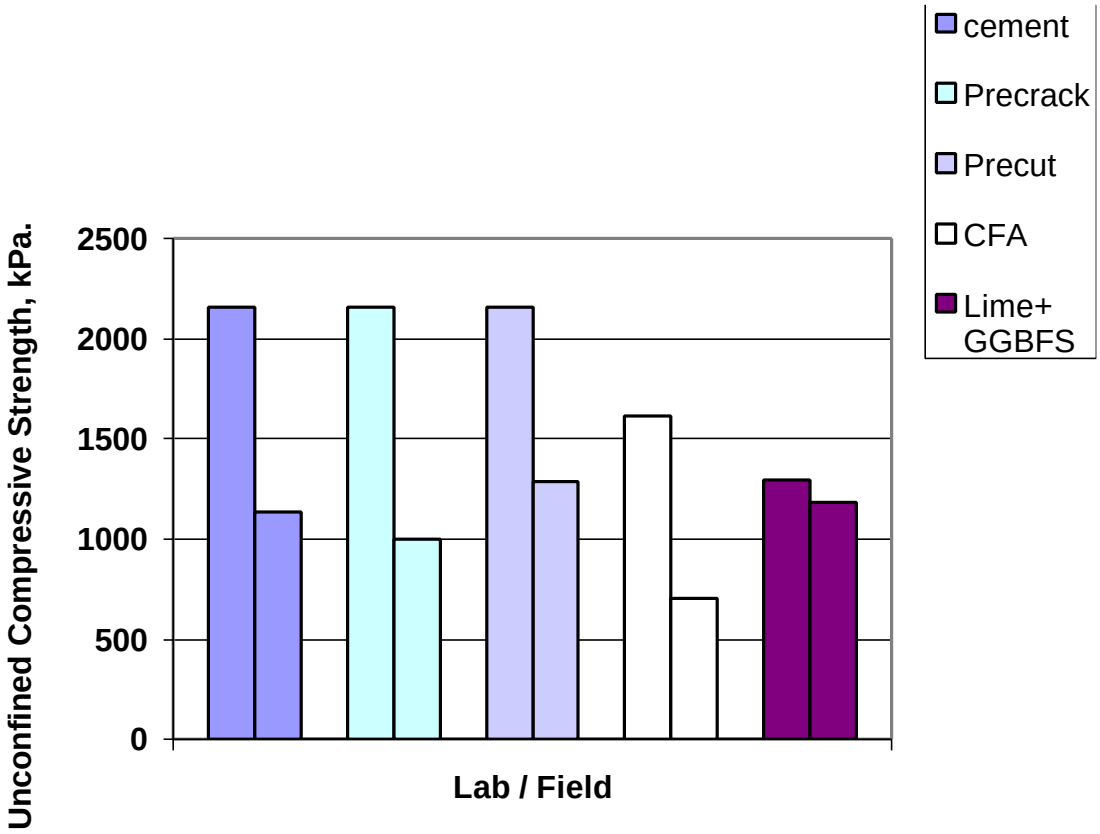

Figure 5.1 Comparison of compression strengths of laboratory prepared and field mixed Proctor samples tested at 7 days. 1 kPa = 0.145 psi

stabilizing agent and water could be incorporated with such ease that the mixed material had passed the Department specification.

5.1.2 In-Place Density Using Sand Cone

Sand cone density listed in Table 4.2, expressed as percent compaction, is plotted against sand cone location (see Figure 5.2). For comparison, density obtained using a Nuclear Density gauge (furnished by the MDOT Project Office) is also plotted in the same diagram. Generally, densities obtained by two independent methods are in agreement, except for in five locations where the sand cone density was significantly lower than the nuclear gauge determination. The sand cone density could be suspect at those locations, due in part to uncertainty in seating the electronic scale on properly leveled support.

A recommendation may be in order here that better density control should be aspired for in future construction. Equally important is that percent compaction shall not be less than 95 percent. A test strip, investigating the type and weight of roller suitable for the soil in question, should dispel those issues regarding uniformity and degree of compaction.

5.1.3 Moisture Content of Mixtures in Test Sections

Again, moisture determined from sand cone samples (by Speedy Moisture Meter) and those obtained from nuclear gauge are plotted in Figure 5.3. Moisture determined using the nuclear gauge appears somewhat uniform from section to section, with moisture values on average 10%. It is important to note that the moisture (determined by Speedy Moisture Meter) in the first subsection, 1A, was high—in the 14 percent range. The relatively extensive cracks in this section, in comparison to the replicate section 3A, is a testimonial for the detrimental effects of excessive moisture in cement-treated material.

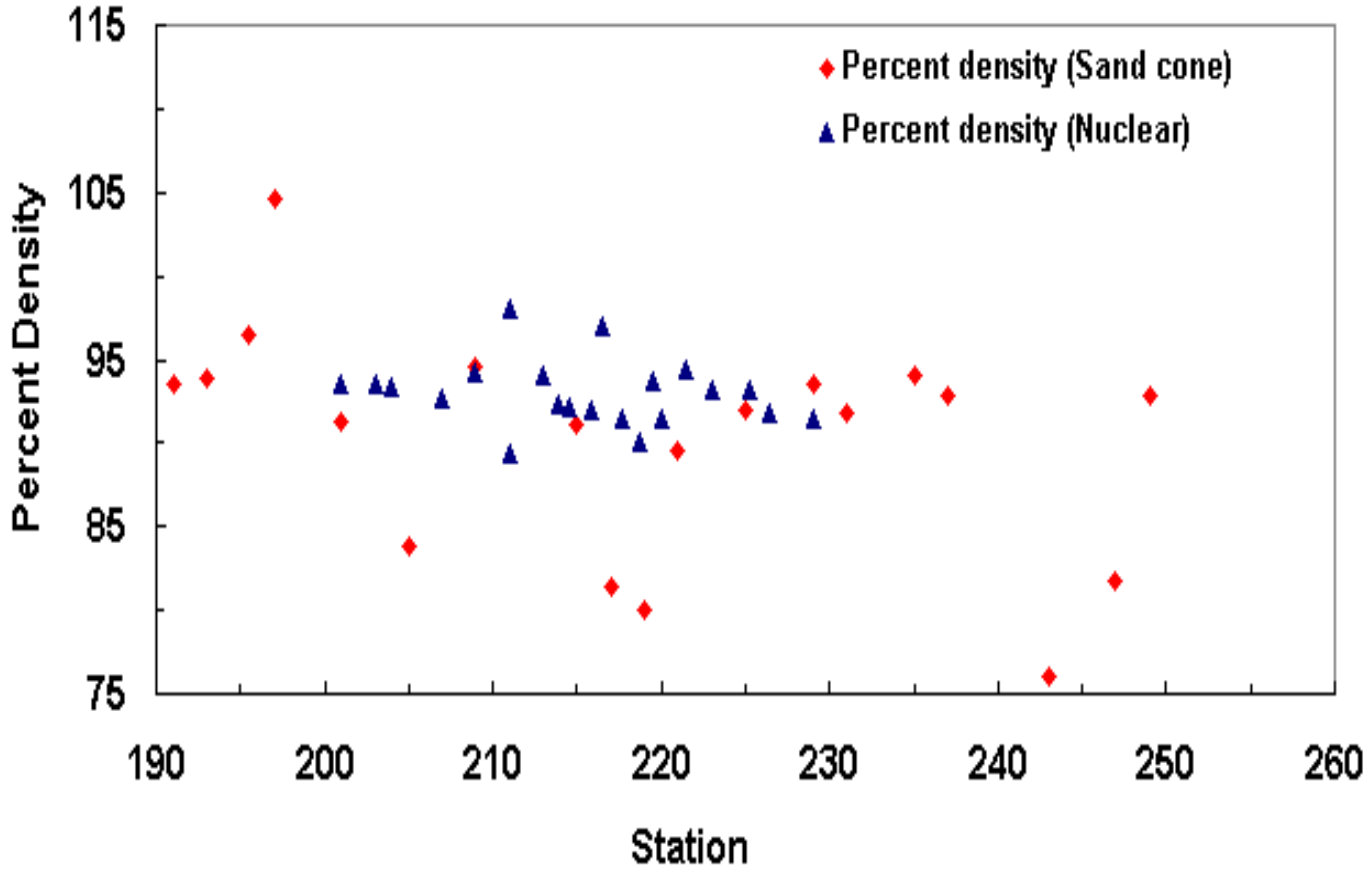

Figure 5.2 Density determined by (i) Sand cone and (ii) Nuclear density device.

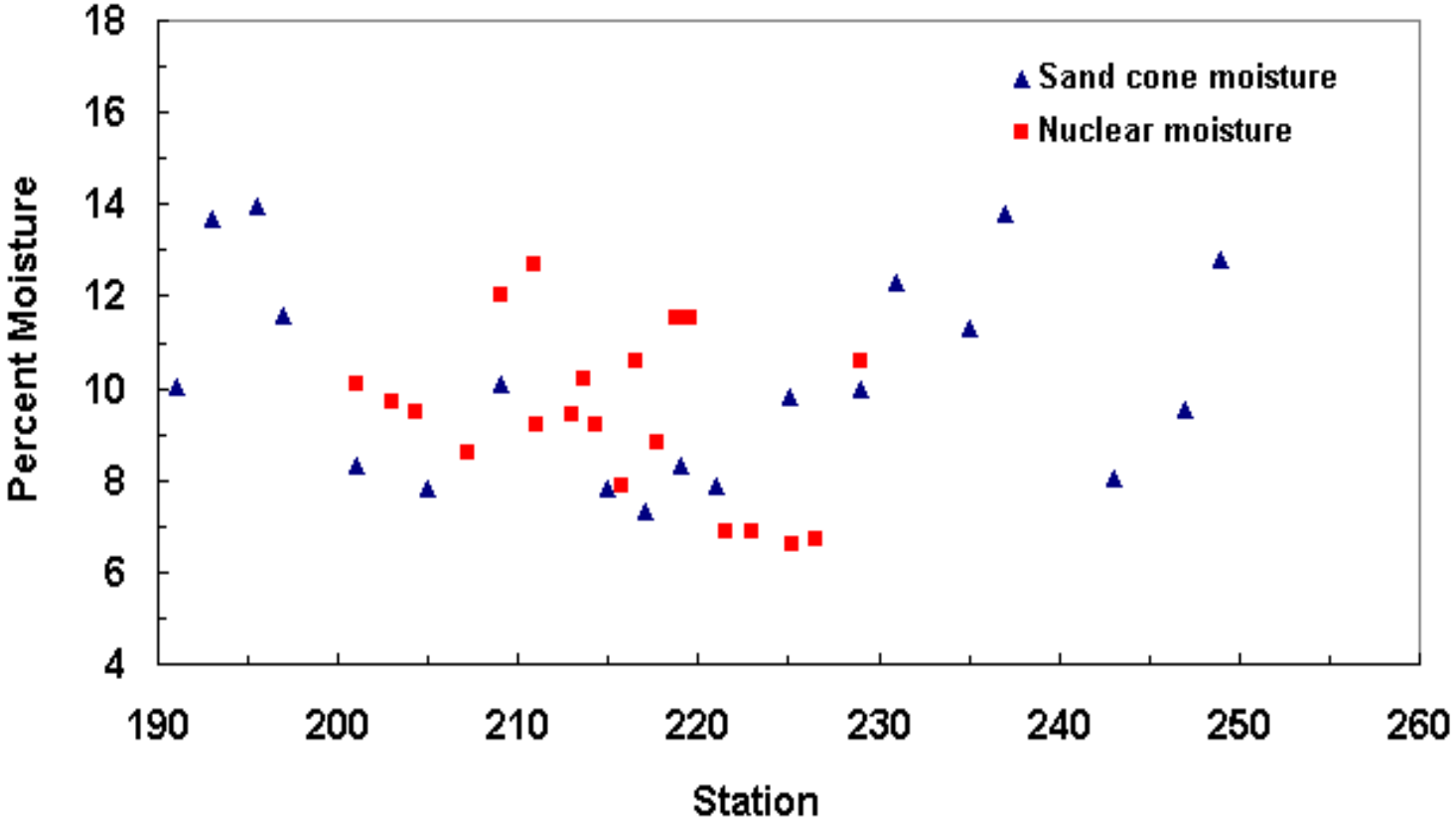

Figure 5.3 Moisture determined by (i) Speedy moisture meter and (ii) Nuclear moisture meter.

5.2 POST CONSTRUCTION EVALUATION TESTS

Described herein are the results of in-place modulus determination at various time intervals, three crack survey results, and finally the strength results – in-place strength by Clegg impact hammer in three successive intervals and core strength at 28 days.

5.2.1 Modulus of Stabilized Subbase

Two devices – geogauge and FWD – were employed in evaluating the modulus of the stabilized layer. Side-by-side tests were planned with geogauge and FWD at seven and 28 days. In addition, geogauge tests were repeated twice, namely, four and 14 days. Tables 4.3 and 5.2 list geogauge and FWD results, respectively.

Note that geogauge measures the modulus directly whereas FWD deflection basins had to be analyzed by a backcalculation routine. MODULUS 5.1 (32) was selected for this purpose. Backcalculation analysis had to be repeated by inputting several E_4/E_5 (subgrade modulus/stiff layer modulus) ratios, e.g., 3, 5 and 10 instead of 50, the default value in MODULUS 5.1. The modulus reported in Table 5.2 is the best in our judgment from a series of runs with different ratios and/or after neglecting the farthest sensor deflections.

Comparing the moduli from the two lists, it is clear that the geogauge modulus is consistently lower than the FWD backcalculated modulus, on average 15 percent. Being an untested device, geogauge moduli need authentication in controlled field trials. It is gratifying to note that the geogauge and FWD moduli exhibit the same trend temporally and spatially. For example, Figure 5.4 depicts the ratio of FWD/geogauge moduli along the roadway. The ratio fluctuates from section to section, with an average value of 7.0.

Another result of interest pertains to FWD modulus decreasing significantly from 7 to 14 days (Table 5.2). The Geogauge modulus shown in Figure 5.5, also decreases slightly these results indeed contradict modulus of samples cured and tested in the laboratory. One plausible explanation for this

Table 5.2 Back calculated moduli of various sections employing deflection measurements.

Section	Station	Moduli, MPa [a]		Average Moduli, MPa [a]		28-Day Average Static Moduli, MPa [a]
		7 Days	28 Days	7 Days	28 Days	
1-A	190+50	2210	2540	2420	1850	220
	191+50	3230	1380			
	192+50	630 [c]	190 [d]			
	193+50	1560	1450			
	194+50	880 [c]	810 [c]			
3-A	210+50	2270	1160			
	211+50	2080	980			
	212+50	3820	3270			
	213+50	2690	2570			
	214+56	1520	1430			
2	201+00	650 [d]	710 [d]	1710	1380	130
	202+00	1170	850			
	203+00	4320 [c]	2160			
	204+00	660 [d]	290 [d]			
	205+00	590 [d]	720 [d]			
	206+00	370 [d]	480 [d]			
	207+00	970	990			
	208+00	3000	1950			
	209+00	740 [c]	940			
1-B	195+50	1540	940	2060	1470	210
	196+50	1630	1340			
	197+50	1980	2670			
	198+50	1810	1660			
	199+50	2120 [c]	600 [c]			
3-B	215+50	2700	1500			
	216+50	1900	1040			
	217+50	380 [d]	3430 [b]			
	218+50	2850	1060			
	219+50	650 [c]	1520			
4	221+00	900 [d]	2040	2810	2380	280
	222+00	2030	434 [d]			
	223+00	3840	330 [d]			
	224+00	4600 [c]	2760			
	225+00	2360	920 [c]			
	226+00	3040	480 [c]			
	227+00	1100	810 [c]			
	228+00	5200	830 [c]			
	229+00	2070	2340			
5	231+00	2690	6900	3090	2640	350
	232+00	6710	4530 [c]			
	233+00	4910 [c]	9960 [b]			
	234+00	5290 [c]	1070			
	235+00	1360 [c]	1900			
	236+00	1850	1960			
	237+00	4110	1010 [c]			
	238+00	2370	1350			
	239+00	830	3760 [c]			
6	241+00	1250	1280	650	700	100
	242+00	700	850			
	243+00	350 [d]	430 [d]			
	244+00	830	680			
	245+00	370	280			
	246+00	410	220 [d]			
	247+00	320	370			
	248+00	2420 [b]	220 [d]			
	249+00	270 [d]	260 [d]			

[a] 1 MPa = 0.145 ksi
[b] Outlier tested according to Chauvenet's criterion
[c] Not considered in the average calculation because of unsatisfactory deflection bowl.
[d] Modulus of treated subgrade larger than the top stabilized layer.

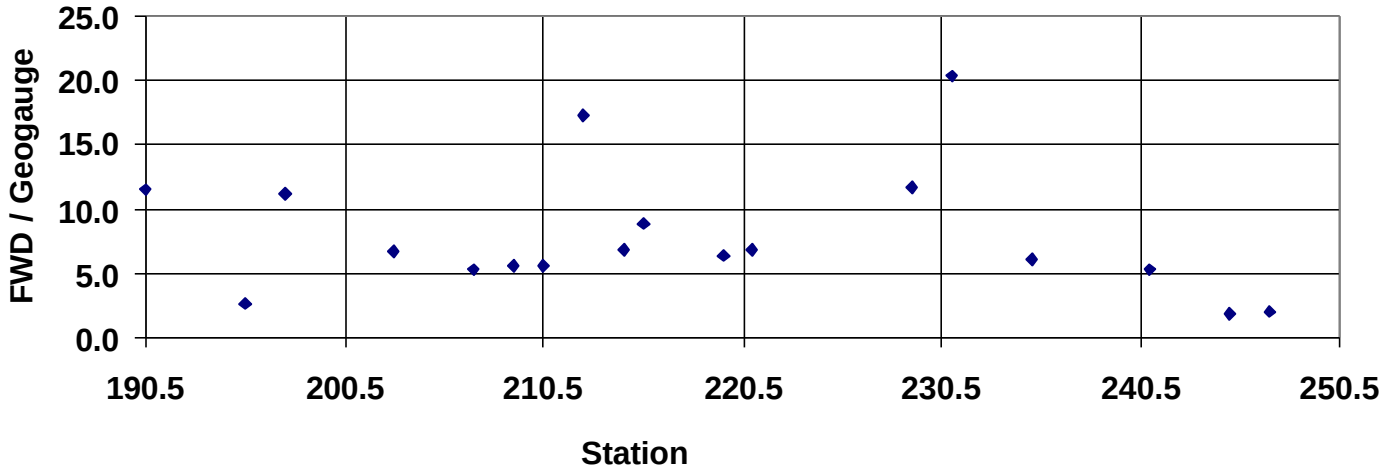

Figure 5.4 Spatial variation of ratio of FWD and geogauge moduli, 28 days.

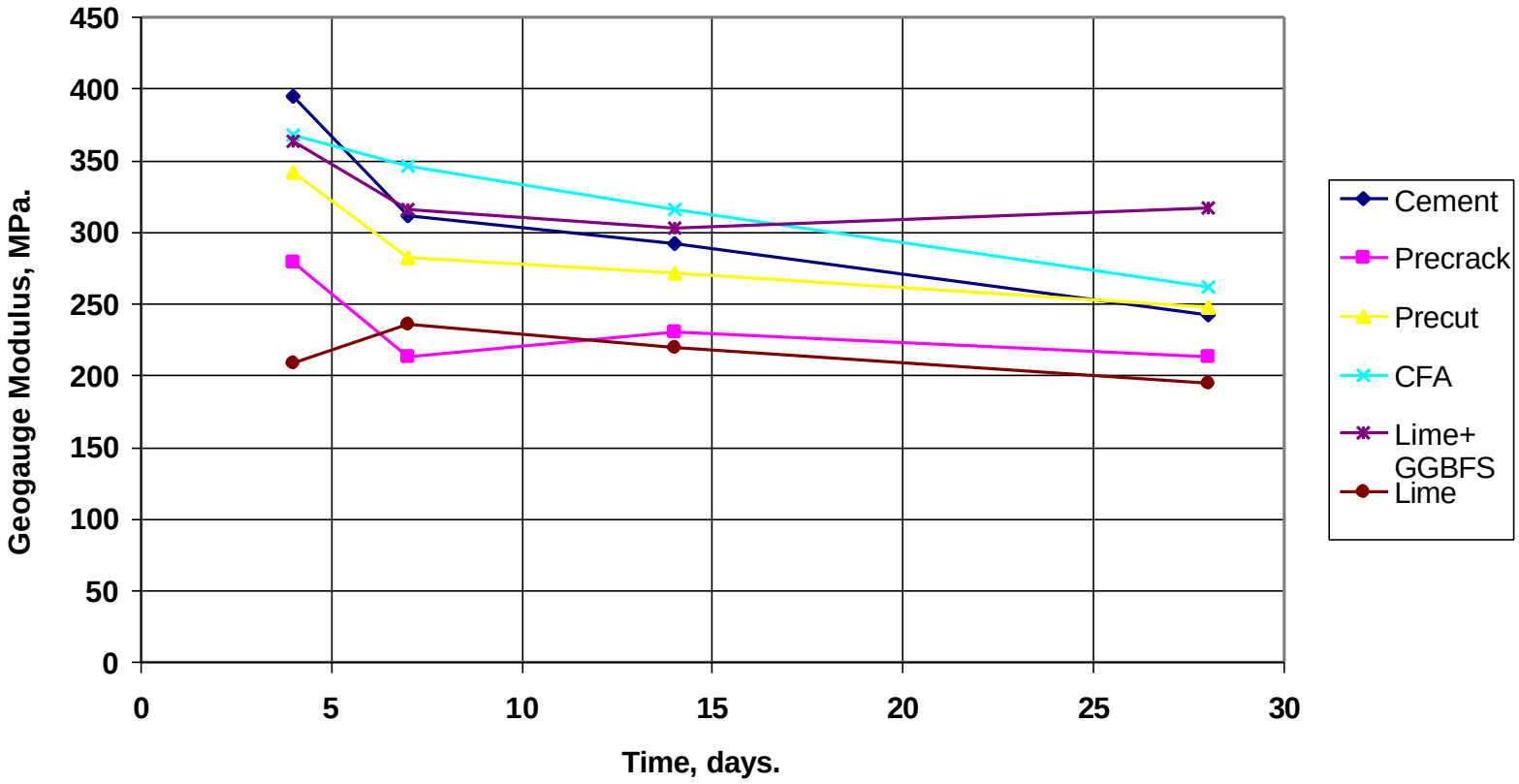

Figure 5.5 Variation of geogauge modulus with time. 1 MPa = 0.145 ksi

anomalous result is that the material in the field, owing to severe desiccation, undergoes damage in the form of microcracks. Internal damage is manifested as modulus decrease.

A comparison of 28-days FWD moduli of different admixture combinations, as shown in Figure 5.6, suggests that,

- The mean value of control cement section, the precracked section and the precut section are statistically the same.
- The lime-fly ash shows the least of all moduli, only 45% of that of the control cement admixture, whereas CFA and lime + GGBFS exhibiting relatively large modulus.

5.2.2 Special Studies of Resilient Modulus

5.2.2.1 Comparison of Static Modulus and Backcalculated Modulus.

Average static moduli for each section determined on 28-day cores, tabulated in Table 5.2, are compared with backcalculated moduli from corresponding sections. There is hardly any correlation between the two sets of moduli. As expected, laboratory static tests on cores results in significantly smaller moduli than the backcalculated values. Overall, the ratio of the static to backcalculated moduli is approximately 0.12, lower than the ratio 0.33 advanced by AASHTO for subgrade soil.(33). Primarily, two factors could be cited for the significantly small static moduli:

- The disturbance resulting from cutting cores, and
- The relatively soft plaster of paris used for capping the cores

resulting in large deformation and, in turn, small modulus

5.2.2.2 Load Transfer Efficiency (LTF) of Precut Grooves

Recognizing that load transfer across precut grooves (and for that matter, cracks also) is crucial for long-term performance, LTEs of several backfilled grooves were determined. FWD deflection measurements were obtained, first with sensors 1 and 2 on both sides of the groove, and

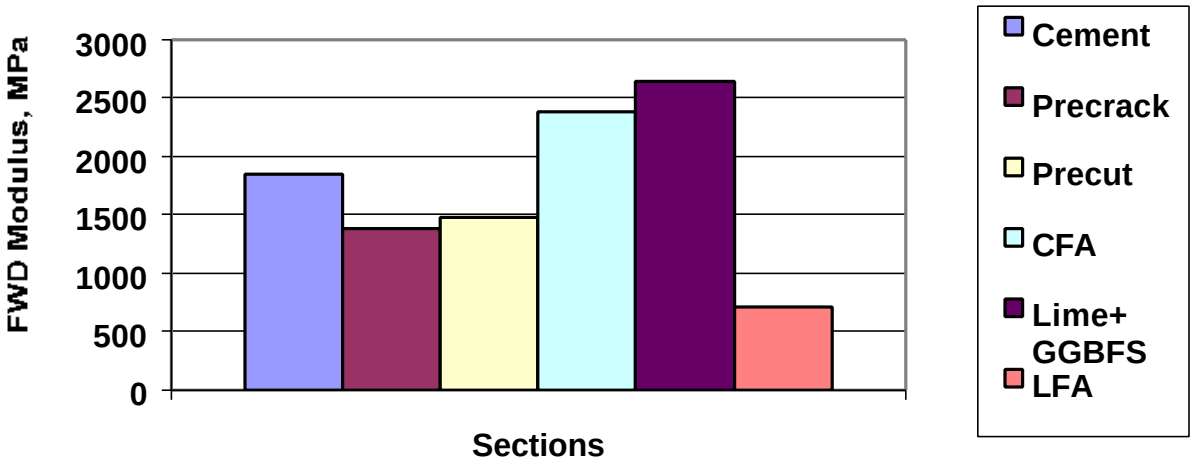

Figure 5.6 Comparison of 28-day FWD modulus of various sections. 1 MPa = 0.145 ksi

second on adjacent uncracked sections. The ratio of the second sensor deflections of the first and second test setups is presumed to provide the load transfer efficiency of the groove. Presented in Table 5.3 are the LTEs of five grooves, measured after 14 days. LTEs of a majority of the grooves tested are below 80%, a target value according to reference 4.

In the British study of Shahid and Thom (19), LTEs measured were of the order of 80%, three months after construction. It may be that as cement hydration progresses, better LTEs could be realized in the precut sections. Nevertheless, the low LTE suggests that an even narrower precut would be desirable for improved performance. The writer recommends that precut groove width be limited to 10mm (3/8 inch) width, as recommended by Shahid and Thom (19).

5.2.3 Cracks in the Stabilized Subbase

Crack lengths categorized and mapped on grid paper were the basis for calculation of effective cracked area, expressed in percent area crack, or simply percent. Evolution of cracks for the six sections is graphed in Figure 4.18. Maximum crack percentage exhibited a range of values with as low as 2.25% in the lime-fly ash section to almost 18.5% in control cement section. All of the sections underwent substantial cracking from 7 to 19 days, with precracked and lime-fly ash sections showing the least increase. Besides inherent shrinkage cracks, extreme hot weather during the 12-day interval could have accentuated crack susceptibility. Between 19 and 28 days, however, the crack density slightly decreased in all of the sections. The 9mm (0.35 inch) precipitation on the twenty-fifth day (see Tables B2 and B7) could have caused closure of some of the shrinkage cracks with a slight decrease in crack density. An examination of the raw data suggests that some cracks have moved down one level in severity, a testimonial that the crack widths have decreased owing to precipitation.

Table 5.3 Load transfer efficiency of precut grooves, 28 days.

Stations	Load transfer efficiency, %
195+55	55
197+53	53
199+53	77
215+52	83
219+52	52

Comparing control cement sections 1A and 3A, the former cracked more, owing primarily to slightly larger moisture content of the mix during compaction as verified during Sand Cone Test (see Figure 5.3). Respectively, sections 1A and 3A moisture contents are 12.2% and 9.3%.

Comparison of crack density in Figure 4.18 shows that lime-fly ash and precracked sections no doubt out-performed the other three sections. That the precut section exhibited nearly three times as much cracks as the precracked section is not an entirely unexpected result, because artificial cracks were introduced in the former at 3m (10 ft) intervals. Why the cement-fly ash section cracked as much as the control section is still an unresolved issue. If laboratory shrinkage studies were an indication, the cement-fly ash section should have cracked less than the control cement section. Under laboratory conditions, the cement-fly ash mixture underwent less drying shrinkage than the cement mixture.

Relying on the crack survey results, a discussion of crack density/severity during the three surveys is presented in Appendix B. Also included in the appendix are photographs of cracks at various stages of its evolution. Relevant conclusions as to effectiveness of various additives/procedures are also included in the appendix. Highlights of these conclusions can be seen in chapter 6.

5.2.4 Compressive Strength of Stabilized Subbase

Compressive strength of in-place stabilized material, determined at three consecutive times employing Clegg hammer, is presented in Table 4.4. Twenty-eight day core strengths are also reported in the table. A discussion of the impact strength values and a comparison of the 28-day strength values of both Clegg hammer and field cores will be presented here. Comparing the Clegg hammer strengths at various ages—four, seven and 28 days—it is noted that the material gained a good part of its strength in four days, with minimal strength increases from four to 7 days

(see Figure 5.7). It could be that extreme hot weather caused accelerated cement hydration, resulting in high early strength. In all of the sections except in the LFA section, strength slightly decreased from seven days to 28 days. This result, though unexpected, agrees with the modulus trend, where it decreased from 14 days to 28 days. The strength of lime-fly ash mixture was relatively small at seven days, and remained low compared to other mixtures; 10998 kPa (145 psi) in 7 days compared to 1011 kPa (147 psi) in 28 days, a negligible increase.

Even more significant is that the strength gain (rate of strength increase) of the LFA mixture is significantly low. These two observations, viewed in light of fewer cracks in LFA section, reinforce the tenet that low strength and/or slow strength gain inhibit shrinkage cracking.

A comparison study reveals that the Clegg hammer registers higher strength than that was obtained from 4-inch cores, both determined after 28 days (see columns 5 and 6 of Table 4.4). Disturbance caused by coring operations and contamination by drilling water used in drilling are the chief factors adversely affecting the strength of cores. In contrast, in the Clegg impact test, the lateral confinement in the field is likely to enhance the strength. Another effect could be that in-place strength (Clegg hammer) is significantly larger than the small sample strength. For comparison purposes, these two sets of results are graphed in Figure 5.8, which captures the general trend in strength variation. For example, the lime-fly ash section is, indeed, weaker than the cement, cement-fly ash and lime-GGBFS sections.

Another comparison is between the 28-day field core strengths and the strength of field-mixed laboratory-molded samples (compare the values in columns 6 and 9 of Table 4.4). Rightly so, the field-mixed laboratory-molded sample strengths are consistently higher than that of the cores, primarily owing to superior compaction imparted by the Proctor hammer. Disturbance resulted from coring operations and moisture contamination are again cited as reasons for low core

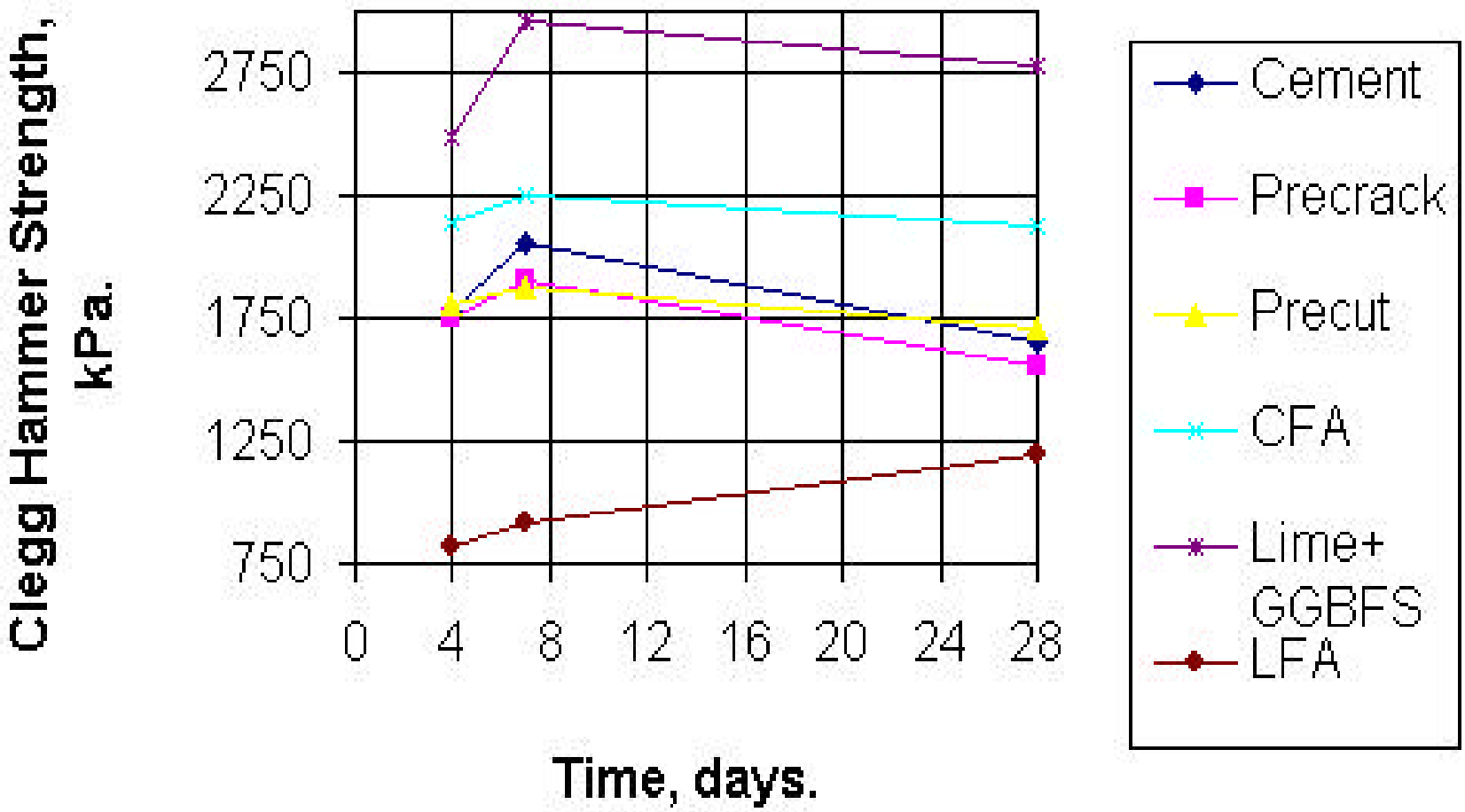

Figure 5.7 Clegg hammer strength with time. 1 kPa = 0.145 psi

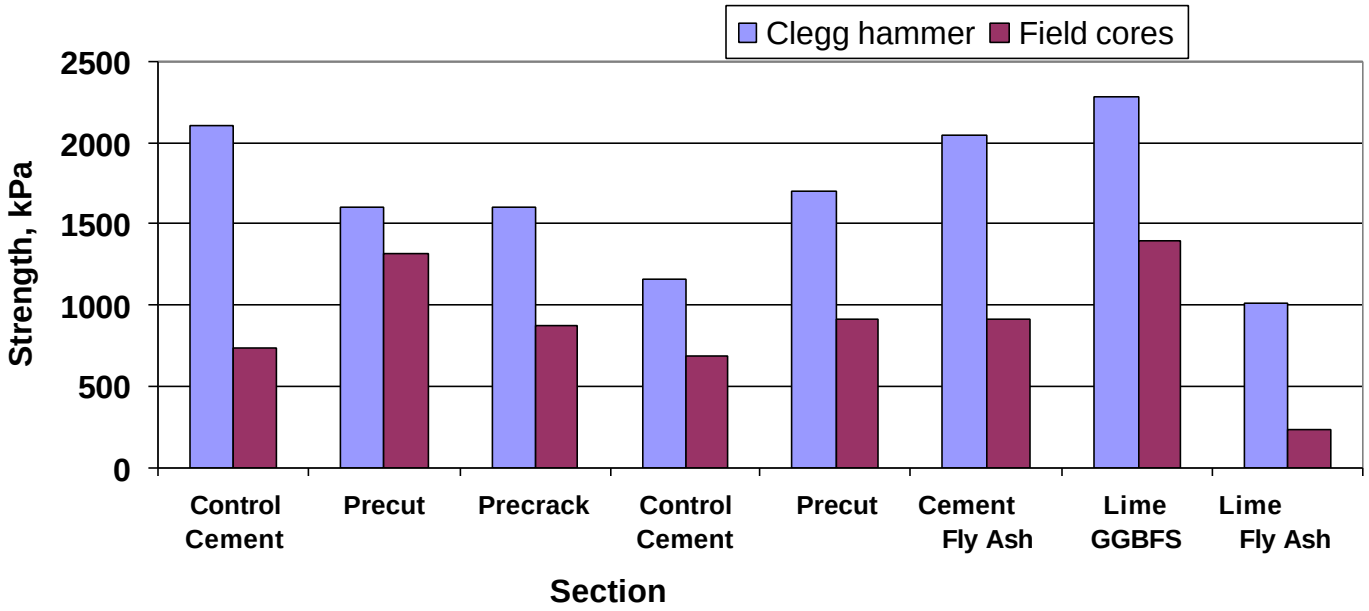

Figure 5.8 Comparison of field core strength with clegg hammer strength, 28 days. 1 kPa = 0.145 psi

strength.

5.2.5 How Modulus/Strength Ratio Affects Shrinkage Cracking?

There is general consensus that low strength material promotes numerous fine cracks; a preferred cracking mode that inhibits reflection cracking. Another measure that seems to bear strongly on shrinkage cracking is the ratio of modulus and strength (34). Reporting his work, Williams hypothesized that lower modulus-strength ratio would be beneficial for alleviating shrinkage cracking. Tentatively, he suggested this ratio not to exceed 2500. In order to validate this tenet, Figure 5.9 is prepared, relating modulus/strength ratio to crack density. It is gratifying to note that the data trend offers some support to Williams' hypothesis that the lower the modulus-strength ratio, the fewer the shrinkage cracks.

5.3 SUMMARY

Construction control test results, such as field density and mix moisture are presented showing their spatial variation. Results show that field mixed material exhibits lower strength than those mixed in the laboratory owing primarily to mix non-uniformity. In place moduli and strength determined at various times suggest that all of the mixtures, except the lime-fly ash, attained full potential in the seven-day period. So far as shrinkage crack are concerned, precracking and lime-fly ash admixture out performed the other admixture/procedures. Relating crack density to the modulus/strength ratio, a weak trend is observed whereby shrinkage cracks decrease with the ratio. The strength gains of different admixture types are discussed, reiterating the assertion that low strength, slow setting mixtures are less prone to shrinkage cracking.

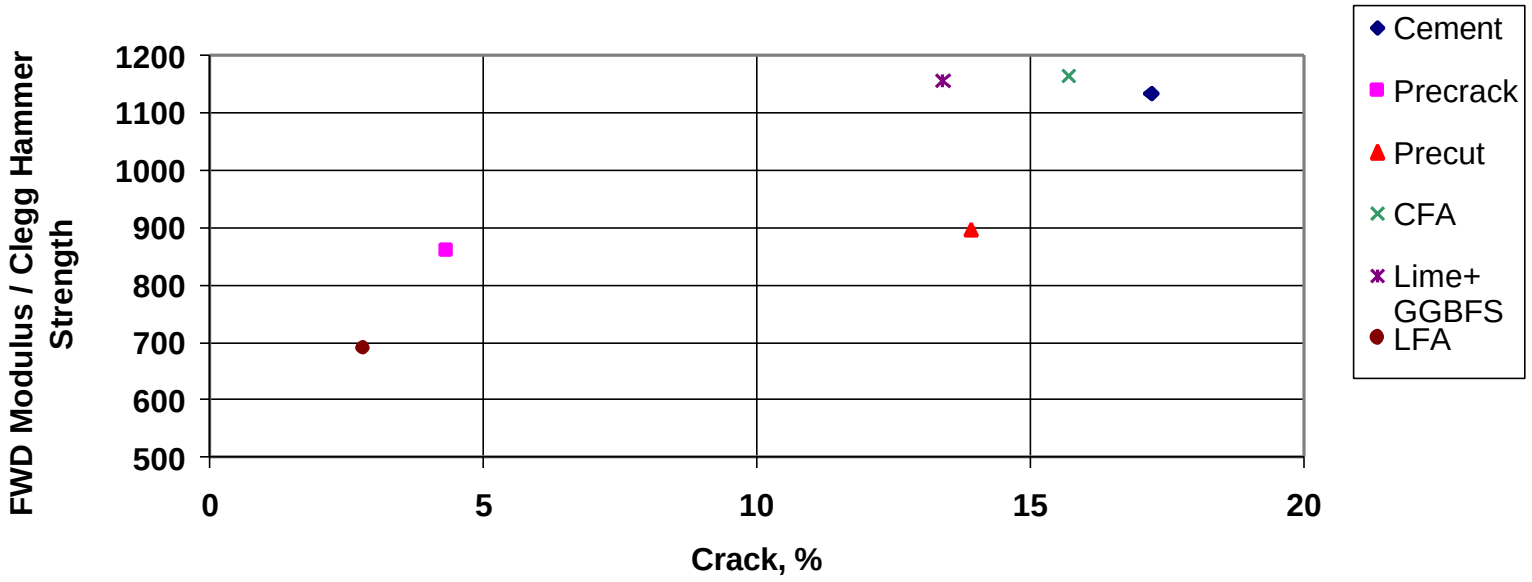

Figure 5.9 Modulus strength ratio plotted against crack density, 28 days.

CHAPTER 6

SUMMARY AND CONCLUSIONS

6.1 SUMMARY

Presented in this first phase report are the preliminary results of the field trial investigating materials and methods for alleviating shrinkage cracks in cement-treated base/subbase layers. Six continuous sections, 305m (1000 ft), are incorporated in Highway #302, with the following admixtures/treatments: cement, precut cement layer, precracked cement layer, cement-fly ash, lime-ground granulated blast furnace slag additive and lime-fly ash. Class 9, group C material is stabilized in place with the additive(s). Tests are conducted in three stages:

- Tests with each mixture for mix proportioning
- Monitoring tests during construction
- Evaluation tests during 28 days after completion of the test sections

The results of these tests are analyzed offering tentative conclusions on mix proportion, construction control specifications and curing procedures to result in a stabilized layer with minimum cracking. For minimizing overall cracking in a pavement surface, in addition to shrinkage cracking of the stabilized layer, potential for reflection cracking (stabilized layer cracks reflecting through the AC surface) should also be dealt with.

What follows are tentative conclusions drawn from the laboratory and field investigations and analysis of test results:

6.2 CONCLUSIONS

6.2.1 Mix Design Tests

- Mix design of cement-treated soil can be accomplished employing ASTM D1633-87,

in which 7-day cured/4 hour water-immersed compressive strength of a 71mm diameter and 142mm high (2.8-inch by 5.6-inch) specimen forms the criterion. Should Proctor samples be used, appropriate strength conversion factor may be applied for correlating to ASTM sample strength. Multiply ASTM Sample strength by 1.3 for equivalent Proctor Sample strength.

• Mix design of slow-setting additive combinations (cement-fly ash, lime-GGBFS and lime-fly ash) may be based on 28-day strength, again following the ASTM D 1633-87 test.

6.2.2 Construction Monitoring Tests

• Large variations in density and moisture are recorded, when constructed in accordance with current specifications.

• Though not conclusive, there is indication that the beginning 61m (200 ft) segment of each construction section had cracked more than the rest, due in part to relatively low density and high moisture.

• Field mixed stabilized material strength on average is 50 percent lower than that of laboratory mixed material.

• Mix uniformity, as determined by material passing a #4 sieve, is satisfactory.

6.2.3 Evaluation Tests

6.2.3.1 *Modulus*

- Moduli determined by geogauge and that backcalculated from FWD deflection measurement show hardly any agreement, the former on average 15 percent of the latter.
- For all of the sections, with the exception of LFA, the 28-day FWD modulus was on average 80 percent of the 7-day modulus. This anomalous result could be attributed to decrease in slab action resulting from extensive cracking.

6.2.3.2 *Shrinkage Cracks*

- All six sections had cracked during the first seven days, the crack density varying from 0.8 percent in precracked section to 10.4 percent in cement-fly ash section.
- Generally, the sections underwent extensive cracking, beginning as early as three days and continuing for three weeks, due in part to persistent dry, hot weather.
- Ideally, low modulus material (flexible with minimal beam action) is desired, however, a low modulus-strength ratio could also be promoted for minimizing shrinkage cracks.
- The full crack-abating potential of cement-fly ash and lime GGBFS could not be realized because of the extreme dry, hot weather and inadequate curing seal provided in the sections. The slow-setting feature of those two mixtures was completely negated by exposing them to extreme weather.

6.2.3.3 *Compressive Strength*

- All five admixture combinations, with the exception of lime-fly ash, attained considerable strength in the first few days, due in part to hot, dry weather.
- In place strength, measured employing Clegg impact hammer, was invariably larger than that from 4-inch cores.
- The 28-day cores showed smaller strengths than the Proctor samples molded from the field mixed material. These results suggest that core strengths should be viewed with caution, as the samples are likely to be disturbed by the mechanical cutting operations. The use of water during the cutting operation might also adversely affect the strength.

6.3 RECOMMENDATIONS

6.3.1 Design and Construction

1. Cement-treated mixture design shall be based on a strength criterion of 2.0 MPa (290 psi), determined in accordance with ASTMD 1633-87. ASTM specifies that sample size be 71mm (2.8 inch) diameter and 142mm (5.6 inch) high, and testing shall be after 7 days moist curing at 72ºF and 4 hours water immersion.
2. Slow-setting admixtures shall be proportioned such that a strength of 2.4 MPa (350 psi) is reached after 28 days moist curing at 72ºF and 4 hours water immersion. (Note: Multiply ASTM sample strength by a factor 1.3 to get Proctor strength). Recommendations 1 and 2 are tentative and should await confirmation based on long-term performance of several test sections.
3. Specifications on density and moisture should be strictly adhered to for quality control. Density requirement shall be increased from 93 percent (as required by MDOT MT-25) to 95 percent compaction or above. Continuous monitoring of density and moisture is required ensuring these measures to be within limits.
4. Adequate curing of the stabilized layer cannot be overemphasized. Curing compound (emulsion) must be applied consistently and before the surface begins to dry. Note the emulsion application varied from section to section in that some sections received adequate emulsion while others barely enough to be effective. Regarding the application time, if the finished surface begins drying due to evaporation of moisture, it must be replenished before the application of curing compound.

5. If excessive moisture loss is detected (by periodic moisture measurement) during the 7-day period, steps should be taken to replenish the moisture loss by spraying additional water.
6. The cement stabilized layer shall be overlaid with asphalt surface as early as practical, not earlier than three days and not exceeding seven days. Considering the slow strength gain asphalt placement may be extended to 14 days for LFA base.
7. Should it be necessary to delay the surface placement, curing seal shall be applied at intervals to alleviate desiccation of the stabilized material.
8. The monitoring tests during construction brought to light an important issue as to how to produce a uniform material. Field mixing is bound to result in spatial variabilities in additive dosage as well as mix uniformity. The strength and modulus test results reported here suggest just that. Mix uniformity may be enhanced during dry mixing by increasing the number of passes to a minimum of four.

6.3.2 Performance

Performance of the six test sections are evaluated based on in place moduli, crack density and compressive strength. From a strength and modulus point of view, lime-fly ash should be suspect, especially if construction is planned for late fall. Shrinkage cracking was the least in lime-fly ash and precracked sections. Precrack techniques, because it satisfies all of the requirements, namely, strength and minimum shrinkage cracking, is recommended for subbase/base construction. The performance of the other four test sections (cement, precut, cement-fly ash and lime-GGBFS) should await further evaluation in the coming years. All these sections are expected to perform satisfactorily from the strength point of view, however, to what extent the pre-existing cracks reflect through the asphalt layers would determine their long term performance.

REFERENCE

1. Crawley, A.B., Memorandum, Cement Kiln Dust-Fly Ash Aggregate Base Course, Project No. 97-0079-02-017-10, November 13, 1997.

2. Uddin, W. "Improved Asphalt Thickness Design for New and Reconstructed Highway Pavements, FHWA/MS-DOT-RD-99-122, Final Report, University of Mississippi, 1999.

3. Little, D. N., T. Scullion, P.B.V.S. Kota and J. Bhuiyan, "Guidelines for Mixture Design of Stabilized Bases and Subgrades", FHWA/TX-45/ 1287-3 F, Texas Department of Transportation, Austin, Texas, October 1995.

4. Kota, P.B.V.S, T. Scullion and D.N. Little, "Investigation of Performance of Heavily Stabilized Bases in Houston, Texas, District", Transportation Research Record 1486, Washington, D.C., 1995.

5. Kader, P., R.G. Baran, and R.G. Gordon, "The Performance of CTB Pavements Under Accelerated Loading-the Beerburrum ALF Trail 1986/87", Research Report AAR No. 158, Victoria, Australia, 1989.

6. Finn, F.N., K. Nair, and J.M. Hillard, "Minimizing Premature Cracking in Asphalt Concrete Pavement", NCHRP 195, Transportation Research Record, Washington, D.C., 1978.

7. Norling, L.T., "Minimizing Reflective Cracks in Soil Cement Pavements: A Status Report of Laboratory Studies and Field Practices", Highway Research Record 442, Washington, D.C., 1973.

8. El-Rahim, A., and K.P. George " Optimum Cracking for Improved Performance of Cement-Treated Bases ", Proceedings, Ninth World Conference on Transport Research, Seoul, Korea, July 2001.

9. George, K.P., "Mechanism of Shrinkage Cracking of Soil-Cement Bases", Transportation Research Record 442, Washington, D.C., 1973.

10. El Halim A.O. ABD, et al., "Effect of Highway Geometry and Construction Equipment on the Problem of Reflection Cracks", Proceedings, Third International RILEM Conference, Reflection Cracking in Pavements, The Netherlands, E & FN Spon, 1996.

11. Scarpas, A., et al. "Finite Element Modeling of Cracking in Pavements", Proceedings, Third International RILEM Conference, Reflection Cracking in Pavements, The Netherlands, E and FN Spon, 1996.

12. Teng, T.C., and J.P. Fulton, "Field Evaluation Program of Cement-Treated Bases", Transportation Research Record 501, Washington, D.C., 1974.

13. El Lahan, A.A., and R.L. Lytton, “A Mechanistic-Empirical Approach for Modeling Reflection Cracking”. Transportation Research Record 1730, Washington, D.C., 2000.

14. Caltabiano, M.A., and R.E. Rawlings, “Treatment of Reflection Cracks in Queensland”, Seventh International Conference on Asphalt Pavements, The University of Nottingham, U.K., 1992.

15. George, K.P., “Minimizing Cracking in Soil-Cement for Improved Performance”, Technical Memorandum, Hitek Engineering Consultants, Inc./PCA, Oxford, Mississippi, January 1998.

16. George, K.P., “Shrinkage Cracking of Soil-Cement Base, Theoretical and Model Studies”, Highway Research Record 351, Washington, D.C., 1971.

17. Kuhlman, R.H., “Cracking in Soil-Cement–Cause, Effect, Control”, Concrete International, Vol. 53, 1992.

18. George, K.P., “Crack Control in Cement-Treated Bases”, Final Report, Civil Engineering Department, The University of Mississippi, 1970.

19. Shahid, M.A. and N.H. Thom, “Performance of Cement Bound Bases With Controlled Cracking”, Proceedings, Third International RILEM Conference on Reflective Cracking in Pavement, The Netherlands, E and FN Spon, 1996.

20. George, K.P., “Minimizing Cracking in Cement-Treated Materials for Improved Performance”, Final Report to Portland Cement Association, HITEK Engineering Consultants, Oxford, Mississippi, February 2000.

21. Colombier, G. and J.P. Marchand, “The Precracking of Pavement Underlays Incorporating Hydraulic Binders”, Proceedings, Second International RILEM Conference on Reflective Cracking in Pavements, E and FN Spon, London, 1993.

22. Lefort, M., “Technique for Limiting the Consequences of Shrinkage in Hydraulic-Binder-Treated Bases”, Proceedings, Third International Conference on Reflective Cracking in Pavements, The Netherlands, E & FN Spon, London, 1996.

23. Yamanonchi, T. and M. Ihido, “Laboratory and In-situ Experiments on the Problem of Immediate Opening of Soil-Cement Base to General Traffic”, Proceedings, Fourth Australia-New Zealand Conference, 1982.

24. Litzka, J., “Cold In-place Recycling on Low-Volume Roads in Austria”, Proceedings, Sixth International Conference on Low-Volume Roads, Transportation Research Board, 1999.

25. Davidson, D.T., et al., “Use of Fly Ash with Portland Cement for Stabilization of Soil”, Highway Research Board Bulletin 198, Washington, D.C., 1958.

26. Kasibati, K. and T.l. Conklin, "Field Performance Evaluation of Cement Treated Bases with and without Fly Ash", Transportation Research Record No. 1440, Washington, D.C., 1994.

27. "High-Volume Fly Ash Utilization Projects in the United States and Canada", Publication No. CS-4446, Electric Power Research Institute Palo Alto, CA, February 1986.

28. Sastry, D. "Improving Soil Cement Characteristics with Fly Ash", Master's Project, Department of Civil Engineering, The University of Mississippi, University, MS, 1998.

29. American Society of Testing and Materials, Annual Book of ASTM Standards, Vol. 04.08, Soil and Rock; Building Stones, ASTM, 1916 Race Street, Philadelphia, PA, 1987.

30. Geogauge Brochure, Humboldt Mtg. Co., Norridge, IL, 2000.

31. Okamoto, P.A., et al., "Nondestructive Tests for Determining Compressive Strength of Cement-Stabilized Soils", Transportation Research Record 1295, TRB, National Research Council, Washington, D.C., 1990.

32. Y.J. Chou, and R.L. Lytton, "Accuracy of Consistency of Backcalculated Pavement Layer Moduli", Transportation Research Record 1293, TRB, National Research Council, Washington, D.C., 1993.

33. AASHTO Guide for Design of Pavement Structures, American Association of State Highway and Transportation Officials, Washington, D.C., 1993.

34. Kolias, S. and R.I.T. Williams, "Cement-Bound Road Materials: Strength and Elastic Properties Measured in the Laboratory", TRRL Supplementary Report 344, Transport Road Research Laboratory, U.K., 1978.

APPENDIX A1

TENTATIVE MIX DESIGN CRITERIA FOR CEMENT-TREATED SOIL, CEMENT-FLY ASH AND LIME-GGBFS

MDOT Design (MT-25) for cement-treated soil for subbases calls for a 7-day unconfined compressive strength of 2.7 MPa (400 psi), employing Proctor samples. A telephone survey of several states suggests that the present trend in mix design is to lower cement content with the tenet that a reduction in strength will produce a reduction in shrinkage cracking. Georgia DOT makes use of 3.1 MPa (450 psi) 7-day strength on Proctor samples for mix design. The requirement in Louisiana varies from 1.7 to 2.4 kPa (250 to 350 psi). With due consideration to these specifications, a strength of 2.6 MPa (380 psi) on Proctor-size samples is proposed. Translating this to ASTM size samples 71mm by 142mm (2.8 inch by 5.6 inch) would require a strength reduction to account for size-effect. Our tests show that, with a height-to-diameter ratio of 2:1, ASTM samples test on average 23% less than Proctor samples. Accordingly, a strength criterion (7-day curing at 72ºF followed by 4-hour water immersion) of 2.0 MPa (290 psi) is proposed for ASTM samples.

For slow-setting mixtures like cement-fly ash and lime-GGBFS mixtures, a 28-day strength criterion is desired, as for lime-fly ash. MDOT strength requirement for lime-fly ash mixtures is 3.4 MPa (500 psi) after 28-day curing at elevated temperatures. Because room temperature curing is adequate for the above-mentioned two mixtures, a lower strength would suffice. A 2.7 MPa (400 psi) Proctor strength at 28 days could be suggested, which would translate to 2.1 MPa (305 psi), when ASTM samples are used; however, our experience with cement-fly ash and lime-GGBFS are limited, and with the reasoning that a strength of 1.4 MPa (200 psi) in 7 days would be warranted for accommodating construction traffic, the 28-day criterion is set at 2.4 MPa (350 psi) on ASTM samples, or 455 psi for Proctor size samples.

APPENDIX A2

SAMPLE CALCULATION OF CRACK DENSITY

Section 193+50 to 194+50 (100 ft. long and 14 ft. wide) See Table B2, row 4

Weighted crack area = (0 * 0.2 + 110 * 0.5 + 205 * 0.75 + 34 * 1) ft (length) * 1 ft (effective width[a])

= 242.75 square feet

Weighted crack or crack density, % = 242.75 square feet * 100/(100 ft. (long) * 14 ft. (wide))

= 17.3%

[a]Assumed that the affected width is one foot

APPENDIX B

SUMMARY OF CRACK SURVEY CONDUCTED AT SEVEN, 19 AND 28 DAYS

B.1 INTRODUCTION

As discussed in chapter 4, a three-man crew, mapping cracks three, seven, 19 and 28 days since construction, surveyed the test sections. The data is aggregated and plotted in Figure 4.18.

As regards to shrinkage cracking caused by desiccation, weather conditions and curing (to prevent moisture loss) play a crucial role in the outcome. Dry, hot weather, with highs around 100°F prevailed for more than three weeks after construction. The maximum and the minimum temperatures beginning 8/17/00 through the following 28 days are tabulated in Table B.1. The only precipitation received during this period was 10mm (0.35 inches) on the twenty-fifth day.

Another issue is related to adequacy of curing. Specifications called for priming the finished surface with EPR-1 emulsion applied at the rate of 0.15 gallons per square yard. From section to section, the emulsion quantity varied somewhat, as illustrated by the color of the sprayed surface. Figure B1 shows noticeable contrast between adjacent sections, one receiving adequate emulsion (background) and the other barely enough to be effective (foreground).

B.2 CRACK SURVEY RESULTS

A breakdown of cracks of four different severity levels compiled in three surveys is presented in Tables B2 to B7. What follows is a section-by-section discussion of the crack survey results: 7 day, 19 day and 28 day crack data.

B.2.1 Control Cement (Station 190+50 to 194+50) Section 1A

On average 8.1 percent low severity cracks were observed after seven days, which increased to 17.2 percent by the nineteenth day (see Table B2). The medium severity cracks were twice as numerous as the low severity cracks. No substantial change was observed at 28 days except that

Table B1 Climatological data for the project site (weather station: Memphis International Airport); August and September of 2000

Date	Maximum Temperature ^{o} F	Minimum Temperature ^{o} F	Average Temperature ^{o} F	Precipitation (inches)
8-17	103	78	91	0.00
8-18	94	75	85	**T***
8-19	90	70	80	0.00
8-20	89	71	80	0.00
8-21	99	73	86	0.00
8-22	100	77	89	T
8-23	98	75	87	0.00
8-24	94	77	86	0.00
8-25	96	76	86	0.00
8-26	102	77	90	0.00
8-27	103	80	92	0.00
8-28	104	77	91	0.00
8-29	106	77	92	0.00
8-30	107	79	93	0.00
8-31	103	81	92	0.00
9-1	102	77	90	0.00
9-2	101	77	89	0.00
9-3	101	77	89	0.00
9-4	102	77	90	0.00
9-5	78	71	75	0.00
9-6	91	68	80	0.00
9-7	82	67	75	0.08
9-8	82	70	76	T
9-9	86	75	81	T
9-10	91	75	83	T
9-11	95	76	86	T
9-12	88	71	80	0.35
9-13	91	69	80	0.00
9-14	96	67	82	0.00
9-15	82	65	74	0.00
9-16	79	57	68	0.00
9-17	83	54	69	0.00

T* – Trace Precipitation Amount.

Figure B1 Section 1B (precut) in the foreground and section 2 in the background. Contrast in emulsion application.

Figure B2. Medium severity crack in section 1A, control cement, nineteen days.

Table B2. Crack survey results of control cement, sections 1A and 3A (5.5 percent cement).

Section	Station	7 Days					19 Days					28 Days				
		Crack length, ft				Weighted crack, %	Crack length, ft				Weighted crack, %	Crack length, ft				Weighted crack, %
		Fine	Low	Medium	High		Fine	Low	Medium	High		Fine	Low	Medium	High	
1-A	190+50 to 191+50	0	70	0	0	2.5	0	147	200	0	16.0	0	140	207	0	16.1
	191+50 to 192+50	0	200	0	0	7.1	0	117	239	7	17.5	0	154	206	7	17.0
	192+50 to 193+50	0	388	0	0	13.9	0	77	294	0	18.5	8	158	212	0	17.1
	193+50 to 194+50	0	251	0	0	9.0	0	110	239	0	16.7	0	110	205	34	17.3
Average						8.1					17.2					16.9
3-A	210+50 to 211+50	14	160	0	0	5.9	0	530	0	0	18.9	0	530	0	0	18.9
	211+50 to 212+50	0	37	0	0	1.3	0	617	0	0	22.0	0	617	0	0	22.0
	212+50 to 213+50	0	27	0	0	1.0	0	575	0	0	20.5	0	575	0	0	20.5
	213+50 to 214+50	0	103	0	0	3.7	0	526	0	0	18.8	11	224	0	0	8.2
Average						3.0					20.1					17.4

1 feet = 0.3 meters.

some medium severity cracks reverted to low severity level. A typical medium severity crack is shown in Figure B2.

Due primarily to the precipitation three days before the 28-day survey, the crack density slightly decreased. Reversal of desiccation could be the primary reason for this slight decrease in crack width, and, in turn, severity level. As can be verified in Table B1, the temperature began to cool down, another reason for the decrease in crack density between 19 and 28 days. Also heavy construction traffic installing the side drains could have caused the crack edges to spall, resulting in crack closure, especially in the travel lane. As will be shown in the ensuing sections, the crack density in all of the six sections decreased slightly from 19-day to 28-day surveys.

B.2.2 Control Cement (Station 210+50 to 214+50) Section 3A

With very little cracks observed at 7 days, on average 3 percent, they increased dramatically to 20.1 percent at 19 days (see Table B2). Unlike in section 1A, all of the cracks remained at low severity level even at 19 days, however. Preventing early (first seven days) cracks would seem desirable from the point of view of keeping the crack width in check. For the same general reasons, as discussed before, the crack density at 28 days decreased to 17.4 percent, a 2.7 percent change.

B.2.3 Precut (Station 195+50 to 199+50) Section 1B

Mostly low severity cracks appeared along the precut grooves at 7 days (see Table B3). Shown in Figure B3 is a typical transverse crack aligned with a precut groove. At 19 days, however, some transverse cracks attained medium severity level, with crack density increasing to 14.8 percent. Some low severity cracks reverted to the fine category, with very little change in the 28-day crack density. It is noteworthy that emulsion tends to flow under traffic causing further closure of cracks.

Table B3. Crack survey results of precut cement, sections 1B and 3B (5.5 percent cement).

Section	Station	7 Days					19 Days					28 Days				
		Crack length, ft				Weighted crack, %	Crack length, ft				Weighted crack, %	Crack length, ft				Weighted crack, %
		Fine	Low	Medium	High		Fine	Low	Medium	High		Fine	Low	Medium	High	
1-B	195+50 to 196+50	0	286	0	0	10.2	0	334	38	0	14.0	71	272	29	0	12.3
	196+50 to 197+50	0	256	0	0	9.1	0	263	86	7	14.50	45	228	103	0	14.3
	197+50 to 198+50	0	301	3	0	10.9	0	281	116	0	16.3	62	236	137	0	16.7
	198+50 to 199+50	0	264	0	0	9.4	0	363	23	0	14.2	26	331	47	0	14.7
Average						9.9					14.8					14.5
3-B	215+50 to 216+50	128	240	0	0	10.4	8	460	0	0	16.5	294	286	0	0	14.4
	216+50 to 217+50	0	255	0	0	9.1	0	468	0	0	16.7	117	351	0	0	14.2
	217+50 to 218+50	0	198	0	0	7.1	0	270	126	10	17.1	113	193	90	0	13.3
	218+50 to 219+50	0	132	0	0	4.7	0	386	54	0	16.7	224	191	25	0	11.4
Average						7.8					16.8					13.3

1 feet = 0.3 meters.

Figure B3 Transverse crack along a precut groove, section 1B, seventh day.

B.2.4 Precut (Station 215+50 to 219+50) Section 3B

As in section 1B, mostly low severity transverse cracks appeared along the grooves, with 7.8 percent overall cracking in 7 days. By the next survey on the 19th day, the crack density had increased to 16.8 percent, with very few transverse cracks widening to medium severity level. With some low cracks healing between 19 to 28 days, and a few of the medium cracks reverting to low severity, the crack density decreased from 16.8 to 13.3 percent. This trend was observed in Section 3A as well.

B.2.5 Precrack (Station 201+00 to 209+00) Section 2

The surface had very few cracks, with all of them of fine category or low severity (see Table B4). A few transverse and longitudinal cracks were observed at 19 days, again of low severity, and some fine as well. Figure B4 shows the intersection of transverse and longitudinal low severity cracks. As discussed in a previous section, the 28 day crack density was lower than the 19 day value – 4.8 percent compared to 5.1 percent.

B.2.6 Cement-Fly Ash (Station 221+00 to 229+00) Section 4

The first 61m (200 ft) had unusually high crack density, 15.7 percent in 7 days (see Table B5). By the 19th day, the section had numerous cracks, with the first 61m (200 ft) exhibiting some high severity cracks, with a crack percentage above 22 percent and the remaining 183 m (600 ft) showing average crack density at 16.6 percent. A high severity crack after 28 days is portrayed in Figure B5. With extensive desiccation cracking, the 10mm (0.35 inch) rain helped to alleviate the crack density to almost 15.9 percent. Cement-fly ash being a slow-setting cemetitious product, continued cementation of soil with the availability of moisture

could be a reason for the significant decrease in crack density. Crack closure of this nature is

Table B4. Crack survey results of precracked cement, section 2 (5.5 percent cement).

Section	Station	7 Days					19 Days					28 Days				
		Crack length, ft				Weighted crack, %	Crack length, ft				Weighted crack, %	Crack length, ft				Weighted crack, %
		Fine	Low	Medium	High		Fine	Low	Medium	High		Fine	Low	Medium	High	
# 2	201 to 202	39	0	0	0	0.6	162	69.3	4	0	5.0	206	25.41	4	0	4.1
	202 to 203	11	0	0	0	0.2	157	67.12	0	7	5.1	206	25.48	0	0	3.9
	203 to 204	75	4	0	0	1.2	191	81.77	0	0	5.6	243	29.98	0	0	4.5
	204 to 205	13	33	0	0	1.4	198	84.94	0	0	5.9	252	31.15	0	0	4.7
	205 to 206	12	0	0	0	0.2	123	52.87			3.7	157	19.38	0	30	5.1
	206 to 207	53	0	0	0	0.8	156	66.73			4.6	198	24.47	0	24	5.4
	207 to 208	80	0	0	0	1.1	200	85.54			5.9	254	31.36	0	0	4.7
	208 to 209	85	4	0	0	1.4	175	75.04			5.2	223	27.52	30	0	5.8
Average						0.8					5.1					4.8

1 feet = 0.3 meters.

Figure B4 Transverse and longitudinal cracks in section 2 (precracked), nineteenth day.

Figure B5 High severity longitudinal crack in section 4, cement – fly ash, 221 + 50, nineteenth day.

Table B5. Crack survey results of 3.5% cement and 8% flyash, section 4.

Section	Station	7 Days					19 Days					28 Days				
		Crack length, ft				Weighted crack, %	Crack length, ft				Weighted crack, %	Crack length, ft				Weighted crack, %
		Fine	Low	Medium	High		Fine	Low	Medium	High		Fine	Low	Medium	High	
# 4	221 to 222	0	375	58	0	16.5	0	311	124	34	20.2	67	294	91	22	17.9
	222 to 223	0	417	0	0	14.9	0	460	161	0	25.1	107	378	102	12	21.4
	223 to 224	0	243	12	0	9.3	0	315	97	0	16.4	78	266	68	0	14.3
	224 to 225	0	245	12	0	9.4	0	374	15	0	14.2	81	276	15	17	13.0
	225 to 226	0	175	0	18	7.5	0	342	41	26	16.3	55	243	80	31	16.0
	226 to 227	0	207	0	0	7.4	0	225	159	0	16.6	76	103	205	0	15.7
	227 to 228	31	262	0	4	10.1	12	332	107	0	17.8	152	207	92	0	14.5
	228 to 229	0	216	0	0	7.7	0	335	119	0	18.3	192	143	119	0	14.2
Average						10.4					18.1					15.9

1 feet = 0.3 meters.

often referred to as “crack healing”.

Why the cement-fly ash section cracked more than the other section is still not clear. Laboratory studies show this combination undergoing drying shrinkage somewhat less than that of the control cement mixture. Apparently this was not to be the case in the field because of inadequate curing, and especially deficiency in emulsion application. Inadequate curing, aggravated by the dry hot weather of the first 25 days, had caused the cement-fly ash mixture to crack more than its cement counterpart. A recommendation here is to provide for adequate curing while the cementitious reaction continues to impart cementing action.

B.2.7 Lime-GGBFS (Station 231+00 to 239+00) Section 5

With only 4.3 percent cracks at 7 days (all of it of low severity), crack density increased to 14.6 percent by the 19th day (see Table B6). The relatively large increase in cracks, especially in the first 30m (100 ft) could be attributed to this segment gaining high strength, as can be verified in Table 4.4. The average strength measured for this segment was 3601 kPa (522 psi). We can only speculate why the material gained much higher strength relative to the rest of the section. It may be that a disproportionate amount of additive (lime and/or GGBFS) was dropped inadvertently from the tanker. Figure B6 presents a view of random cracks at 14 days. As in other sections, the 28-day crack density decreased slightly from the 19-day value, 14.6 percent to 14.1 percent.

B.2.8 Lime-Fly Ash (Station 246+00 to 254+00) Section 6

As originally planned, the section was to start at 241+00 and end at 249+00. It was realized, after 7 days, that the first 152m (500 ft) of the test section had badly cracked (7.3 percent) compared to the second 152m (500 ft) only 2.1 percent (see Table B7). Figures B7 and B8 show respectively, medium and severe cracks in LFA sections after 19 days. High moisture content (see Figure 5.3), and, in turn, low density (see Figure 5.2) could be the primary reason for this excessive cracking.

Table B6. Crack survey results of 2% lime and 6% GGBFS, section 5.

Section	Station	7 Days					19 Days					28 Days				
		Crack length, ft					Crack length, ft					Crack length, ft				
		Fine	Low	Medium	High	Weighted crack, %	Fine	Low	Medium	High	Weighted crack, %	Fine	Low	Medium	High	Weighted crack, %
# 5	231 to 232	4	109	0	32	6.2	0	332	108	32	19.9	5	324	108	35	19.9
	232 to 233	0	113	0	0	4.0	0	382	20	0	14.7	0	337	65	0	15.5
	233 to 234	0	222	0	6	8.4	0	218	145	28	17.6	0	207	156	28	17.8
	234 to 235	0	172	0	0	6.1	0	306	78	0	15.1	46	231	107	0	14.6
	235 to 236	30	75	0	20	4.5	0	325	37	20	15.0	116	198	48	20	12.7
	236 to 237	15	91	0	0	3.5	0	191	101	0	12.2	35	128	129	0	12.0
	237 to 238	0	22	0	16	1.9	0	299	20	16	12.9	39	253	27	16	12.2
	238 to 239	0	0	0	0	0.0	0	236	18	0	9.4	57	179	18	0	8.2
Average						4.3					14.6					14.1

1 feet = 0.3 meters.

Figure B6. Medium severity crack in section 5, lime – GGBFS, nineteenth day. Curing compound completely vanished.

Table B7. Crack survey results of 3% lime and 12% flyash, section 6.

Section	Station	7 Days					19 Days					28 Days				
		Crack length, ft					Crack length, ft					Crack length, ft				
		Fine	Low	Medium	High	Weighted crack, %	Fine	Low	Medium	High	Weighted crack, %	Fine	Low	Medium	High	Weighted crack, %
# 6	246 to 247	0	133	4	0	5.0	0	134	0	0	4.8	0	137	0	0	4.9
	247 to 248	0	60	0	0	2.1	0	167	0	0	6.0	0	167	0	0	6.0
	248 to 249	0	36	0	0	1.3	0	121	0	0	4.3	0	121	0	0	4.3
	249 to 250	0	0	0	0	0.0	74	0	0	0	1.1	0	74	0	0	2.6
	250 to 251						51	5	0	0	0.9	0	65	0	0	2.3
	251 to 252						0	0	0	0	0.0	0	5	0	0	0.2
	252 to 253						10	0	0	0	0.1	0	10	0	0	0.4
	253 to 254						54	44	0	0	2.3	80	18	0	0	1.8
Average						2.1					2.4					2.8

1 feet = 0.3 meters.

Figure B7. Meandering cracks in lime – fly ash section, 14 days.

Figure B8. High severity cracks in lime – fly ash section, 241 + 50, nineteen days.

Note that percent density was consistently below 85 percent in the first half of the section. Our inspection of the adjacent lime-fly ash construction (185+00 to 190+00 and 250+00 to 260+00) revealed that the first half of section 6 (that is from 241+00 to 245+00) is not typical, and, therefore, a decision was made to abandon this section and annex the segment from 250+00 to 254+00 to the original 246+00 to 250+00 segment, resulting in a 244m (800 ft) section.

The 19-day cracks in the newly constituted section amounts to 2.4 percent, on average. Note that the annexed 122 m (400 ft) segment had very few cracks compared to the other half. Shown in Figure B9 is a view of 28-day fine crack at 250+00. The crack density increased slightly from 19 day to 28 day – 2.4 percent to 2.8 percent. As can be verified in Figure 4.18, the LFA section had the least cracks among all of the sections.

B.3 CONCLUSIONS

1. All six test sections had undergone shrinkage cracking. Seven-day crack density in the cement sections was approximately 6 percent, that is, 6 transverse cracks in a 30m (100 ft) lane. Respectively, the other sections – precracked, cement-fly ash, lime-GGBFS and lime-fly ash – had 0.8, 10.4, 4.3 and 2.1 percent cracks at 7 days.
2. With persistent dry, hot weather for 25 days, the 19-day cracks increased significantly, on average four-fold, except in the lime-fly ash section where the crack increase (7 days to 19 days) was minimal.
3. The crack density remained the same or decreased slightly for having received 10mm (3/8 inch) precipitation, a testimonial for providing adequate curing to promote cemetitious reaction and to control drying shrinkage.

Figure B9. Fine crack in lime – fly ash section, section 6 (alternate), twenty eight days.

4. Low density and/or high moisture tend to increase drying shrinkage, and in turn, shrinkage cracking. The excessive cracking of the first 152m (500 ft) of lime-fly ash section is a testimonial to the detrimental influence of low density/high moisture.

5. Precracking inducing fine cracks in the material tends to reduce shrinkage cracks in stabilized material.

6. Low strength and slow strength gain are the primary ingredients for low crack density. Crack results of lime-fly ash section substantiates this hypothesis.